Master's Thesis

석사 학위논문

Synthesis and characterization of nanocomposite Ni-YSZ anodes by water-in-oil micro-emulsion for solid oxide fuel cells

Yong Min Jung (정 용 민 鄭 容 敃)

Department of Energy Systems Engineering

에너지시스템공학전공

DGIST

2017

Master's Thesis

석사 학위논문

Synthesis and characterization of nanocomposite Ni-YSZ anodes by water-in-oil micro-emulsion for solid oxide fuel cells

Yong Min Jung (정 용 민 鄭 容 敃)

Department of Energy Systems Engineering

에너지시스템공학전공

DGIST

2017

Synthesis and characterization of nanocomposite Ni-YSZ anodes by water-in-oil micro-emulsion for solid oxide fuel cells

Advisor : Professor Kang Taek Lee
Co-advisor : Doctor Chan-Woo Lee

by

Yong Min Jung
Department of Energy Systems Engineering
DGIST

A thesis submitted to the faculty of DGIST in partial fulfillment of the requirements for the degree of Master of Science in the Department of Energy Systems Engineering. The study was conducted in accordance with Code of Research Ethics[1].

11. 17. 2016

Approved by

Professor (Advisor) Kang Taek Lee (Signature)

Doctor (Co-Advisor) Chan-Woo Lee (Signature)

[1] Declaration of Ethical Conduct in Research: I, as a graduate student of DGIST, hereby declare that I have not committed any acts that may damage the credibility of my research. These include, but are not limited to: falsification, thesis written by someone else, distortion of research findings or plagiarism. I affirm that my thesis contains honest conclusions based on my own careful research under the guidance of my thesis advisor.

Synthesis and characterization of nanocomposite Ni-YSZ anodes by water-in-oil micro-emulsion for solid oxide fuel cells

Yong Min Jung

Accepted in partial fulfillment of the requirements for the degree of Master of Science.

11. 17. 2016

Head of Committee _____(인)

Prof. Kang Taek Lee

Committee Member _____(인)

Dr. Chan-Woo Lee

Committee Member _____(인)

Prof. Hochun Lee

MS/ES 정 용 민. Yong Min Jung. Synthesis and characterization of nanocomposite Ni-YSZ anodes by water-in-oil micro-emulsion for solid oxide fuel cells.

201524012 Department of Energy Systems Engineering. 2017. 63p.

Advisors Prof. Kang Taek Lee. Co-Advisors Dr. Chan-Woo Lee.

Abstract

Homogeneously distributed nanocomposite Nickel oxide-yttria stabilized zirconia (NiO-YSZ) powders were synthesized by water-in-oil (W/O) micro-emulsion method for solid oxide fuel cells. The particles synthesized by W/O micro-emulsion procedure with the calcination temperature of 500 ºC, showed fine microstructures with a particle size less than 50 nm. Electrochemical performances were improved by the nanocomposite anode synthesized by micro-emulsion, compared with the results obtained by the conventional anode. The maximum power density of a single cell with micro-emulsion synthesized Ni-YSZ anode showed a higher maximum power density, 359 mW cm^{-2}, compared with that of a single cell composed of conventional Ni-YSZ anode, 204 mW cm^{-2}, at the operating temperature of 850 ºC. The electrode resistance of a single cell fabricated by micro-emulsion had a value of 0.44 Ω cm^2, which was much smaller than the value of conventional cell, 1.14 Ω cm^2, at the same operating temperature with I-V analysis. The enlarged TPB length obtained by the micro-emulsion synthesized Ni-YSZ anode composed of uniformly distributed nano-grains might be the reason of the improved electrochemical performance of a single cell.

Further studies were done to optimize the micro-emulsion procedures for improved cell performances. Three types of micro-emulsion synthesized NiO-YSZ powders, W10N10, W5N15, W0N20, with different alkali concentrations, were discussed. Particle size of W0N20 decreased to 30nm compared with the value of W10N10, around 40nm. Moreover, specific surface area of W0N20 drastically increased to 42.27 m^2/g, from the value of W10N10, 14.98 m^2/g. However, the maximum power density of a single cell was not affected by the alkali concentrations. The electrode resistance of a single cell with W0N20 showed a higher value of 0.65 Ω cm^2, compared with the value of a single cell with W10N10, 0.44 Ω cm^2, at the open circuit voltage with the operating temperature of 850 ^oC, although the particle size of W0N20 is smaller than that of W10N10. The reduced TPB length caused by the agglomeration of too small particles might be the reason of the electrochemical performances of single cells.

Keywords: SOFCs, Nanocomposite, Ni-YSZ, W/O micro-emulsion, Alkali concentrations

List of contents

List of Figures

1. Introduction

Solid oxide fuel cell (SOFC), which directly converts chemical energy into electrical energy, has high energy efficiency and fuel flexibility, and therefore, it is considered as one of promising technology for energy conversion/power generation [1]. SOFCs have other strengths such as low noise and low greenhouse emission, also [2].

One of the research trends of SOFC is enhancing the electrochemical performance of it. Enhancement of the performance of SOFCs is possible by developing new SOFC materials [3, 4, 6], reducing thickness of the electrolyte [5], and optimizing microstructures and materials of the electrode [6, 7, 8].

Nickel-yttria stabilized zirconia (Ni-YSZ) is the most widely used anode material for SOFCs because of high catalytic activity, mechanical stability, and long-term reliability, etc. [1]. Ni is the catalyst for hydrogen oxidation reaction, and the phase for electron conducting [9]. And YSZ acts as the ionic (oxygen ion) conducting phase [10]. The electrochemical reaction of anode is occurred around the triple-phase boundaries (TPBs) where the ionic conducting phase, electron conducting phase, and gas phase contact. Increment of TPB length enhances the electrochemical performances of anodes [11], and to achieve the enlarged TPB length, initial powder morphologies such as particle size and distribution of components, and microstructure of anode which has fine structure and well distributed phases, are important [12, 13, 14, 15].

NiO-YSZ powders could be obtained by the mechanical mixing, conventionally, however, inhomogeneity and large particle size of NiO and YSZ were observed by this method. To synthesize nano-sized and homogeneously distributed particles, various fabrication methods have been applied: co-precipitation [17, 18], sol-gel [19], gel combustion [20], hydrothermal methods [21], polymeric complexing [22] and micro-emulsion [16]. Among these methods, the micro-emulsion procedure is a unique technique because it has thermodynamic stability which makes it possible to obtain formation stability. And micro-emulsion methods can be applied by using low-energy equipment, also [23]. NiO-

YSZ powders were synthesized by applying water-in-oil (W/O) micro-emulsion methods, here. Effects of micro-emulsion on the properties such as anode morphologies and electrochemical performances were discussed in detail. Furthermore, effects of the alkali solution concentrations during micro-emulsion procedures on the properties of single cells were discussed to optimize Ni-YSZ anode and improve cell performance.

2. Research Background

2.1 Fuel cells

2.1.1 Definition and principle of fuel cells

Fuel cells are energy conversion devices which directly convert chemical energy into electrical energy. Fuel cells are composed of a dense electrolyte, which is sandwiched between two porous electrodes; anode (fuel electrode) and cathode (air electrode). The fuel (H_2/ Hydrocarbon) and oxidant (air) are fed into anode and cathode, respectively, and electrochemical reactions are occurred to produce electrical energy.

2.1.2 Types of fuel cells

Fuel cells can be classified into various types depending on the kinds of electrolytes. Among various kinds of fuel cells, the most common types are

- Polymer electrolyte membrane fuel cell (PEMFC)
- Direct methanol fuel cell (DMFC)
- Molten carbonate fuel cell (MCFC)
- Alkaline fuel cell (AFC)
- Phosphoric acid fuel cell (PAFC)
- Solid oxide fuel cell (SOFC)

2.2 Solid oxide fuel cells (SOFCs)

2.2.1 Definition and properties of SOFCs

Solid oxide fuel cells (SOFCs) are all solid-state energy conversion devices which directly converts chemical energy into electricity with high energy conversion efficiency. Moreover, SOFCs are environmental friendly technologies, which can reduce pollutants and noise.

Depending on the geometry, the SOFCs can be classified into planar type and tubular type. Moreover, three types of SOFCs are existed depending on the operating temperature, high-temperature SOFCs (HT-SOFCs), intermediate-temperature SOFCs (IT-SOFCs), and low-temperature SOFC (LT-SOFCs).

A SOFC is composed of porous anode (negative electrode) and cathode (positive electrode) with a dense electrolyte which is sandwiched between the electrodes. The electrolyte acts as an oxygen ion conductor in the case of SOFCs. Hydrogen oxidation reaction (HOR) and oxygen reduction reaction (ORR) are occurred in anode and cathode, respectively.

The state-of-the-art materials for each component of SOFCs are Ni-YSZ cermet (anode), YSZ (electrolyte), and LSM (cathode).

2.2.2 Properties of SOFC anode

Hydrogen oxidation reaction which is occurred at SOFC anode can be expressed by

$$H_2\,(g) + O_O^X \rightarrow H_2O\,(g) + V_O^{\bullet\bullet} + 2e'$$

with Kroger-Vink notation [24].

Ni-YSZ cermet is the state-of-the-art material for anode because of high catalytic activity, long-term reliability, and mechanical stability, etc [1]. Ni acts as an electron conducting phase, and a catalyst for H_2 oxidation reaction [9]. YSZ, which can inhibit the growth of Ni particles during operation, is an ionic (oxygen ion) conducting phase [10].

The electrochemical reaction occurs nearby the triple-phase boundaries (TPBs) at which the gas phase, ionic conducting phase, and electron conducting phase contact, as shown in **Fig. 2.1**. Enlarged TPB length is essential to obtain the enhanced performance of SOFCs [25, 26], therefore, microstructural adjustments have been studied to achieve longer TPB length, as illustrated in **Fig. 2.2**, which shows the effects of particle sizes on the TPB density.

2.2.3 Research trends of SOFC anode

Research trends of SOFC anode are related to enhancement of electrochemical performances and degradation [27, 28, 29]. Various materials have been employed and a number of synthetic techniques have been studied to fabricate SOFC anode which shows improved performances.

Microstructures architect is one of the most effective methods to enhance the electrochemical performance of anode [30]. Homogeneously distributed nanocomposite particles can increase the reaction site, which improve SOFC performances. Therefore, several fabrication methods such as micro-emulsion, sol-gel, co-precipitation, polymeric complexing, hydrothermal methods, and gel combustion have been applied to synthesize nano particles.

2.3 Micro-emulsion

Micro-emulsions, which are liquid mixtures of oil, water, and surfactant, frequently in combination with a cosurfactant, as illustrated in **Fig. 2.3**, are clear, thermodynamically stable, and isotropic. Surfactant forms the interfacial film between hydrophobic phase and hydrophilic phase, and cosurfactant reduces the interfacial tension by ensuring flexibility of interfacial layer, respectively. Micro-emulsions are classified to oil-in-water (O/W) micro-emulsion and water-in-oil (W/O) micro-emulsion by the volume ratio between aqueous phase and oil phase, as shown in **Fig. 2.4**.

Micro-emulsions lead to uniform distribution of nanograins comparing with conventional, mechanical process which only synthesizes powders composed of uniformly distributed nanoparticles, as illustrated in **Fig. 2.5** [16]. Moreover, enlargement of the reaction site can be obtained by micro-emulsion.

2.4 Effects of alkali concentrations

Particle size of the micro-emulsion synthesized powders decrease as the concentration of alkali increase, which can be expressed by several reasons [31, 32].

- Increment of the number density of nucleis leads to decrease of precipitates size.
- Higher pH can stabilize precipitates from dissolution, and therefore, Ostwald ripening, which is the effect expressed in **Fig. 2.6**, is suppressed.

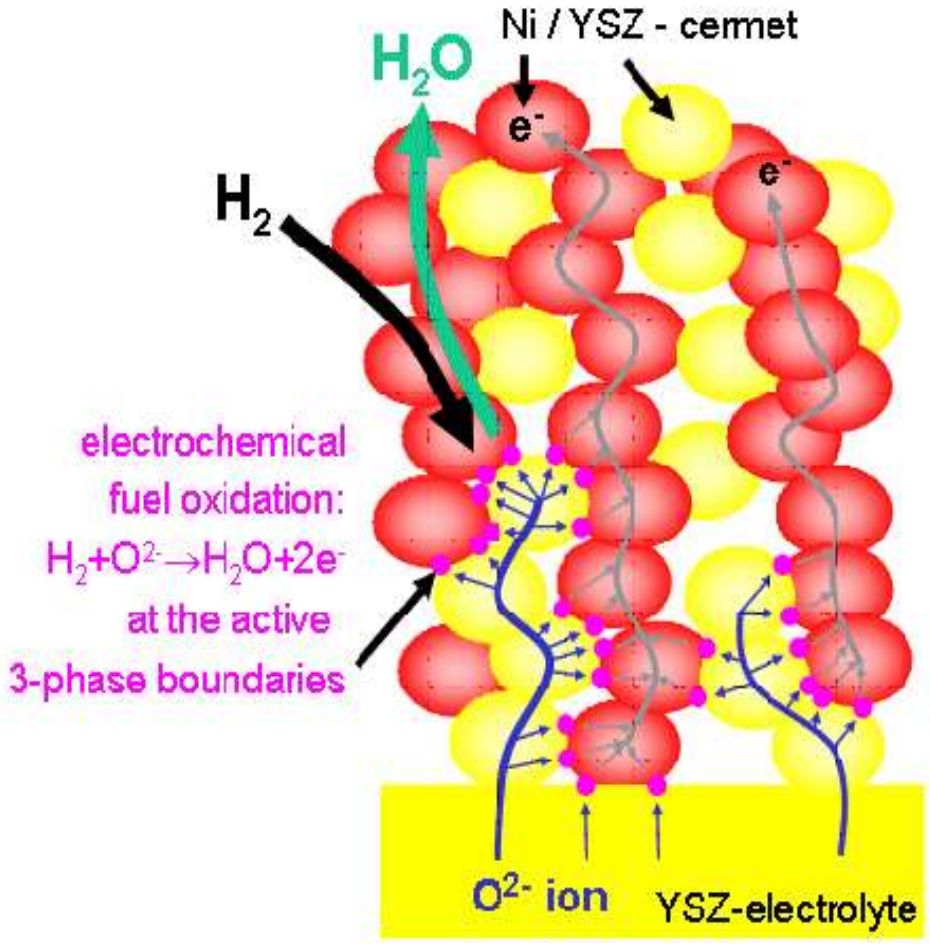

Fig. 2.1. Microstructures of Ni-YSZ anode which shows hydrogen oxidation reaction at the triple phase boundaries.

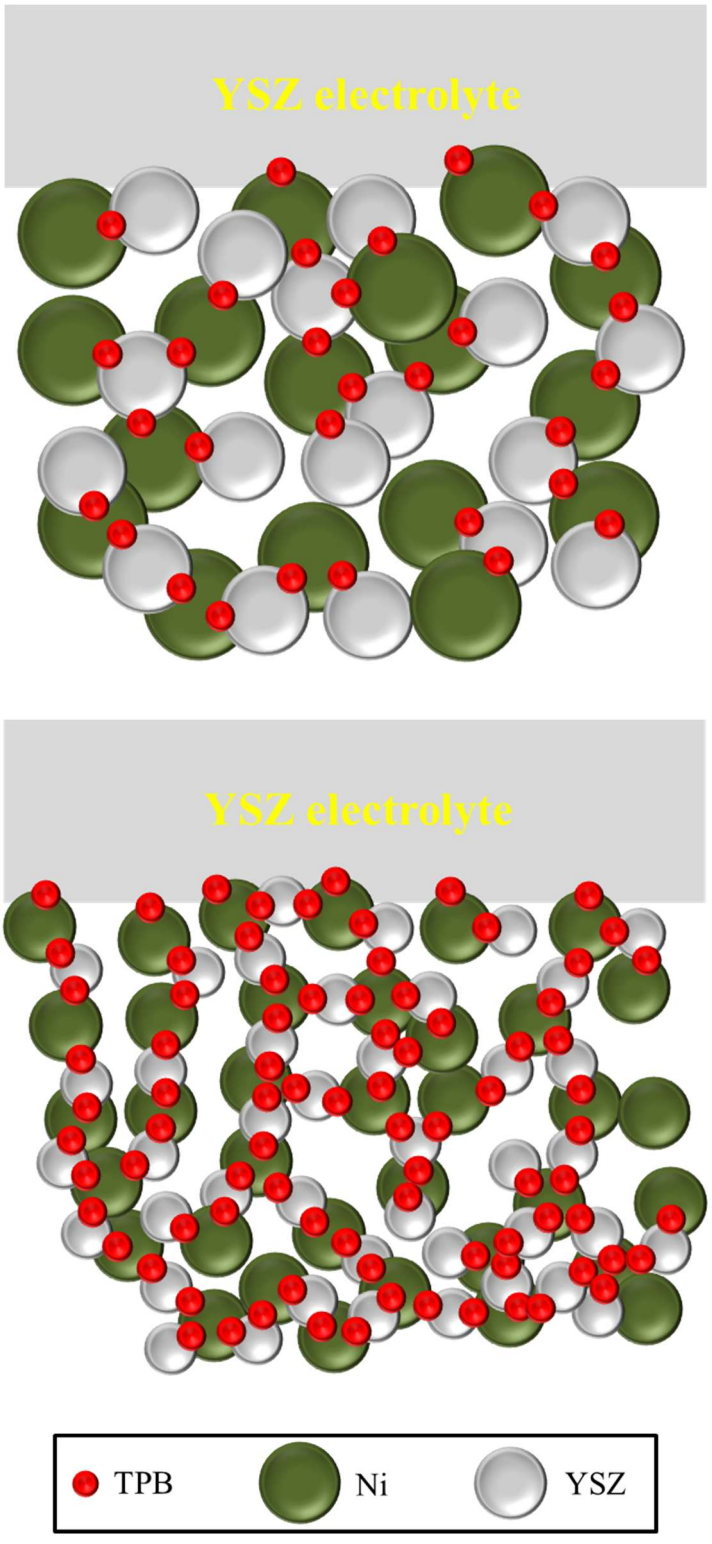

Fig. 2.2. Effect of Ni and YSZ particle size on the length (density) of TPB.

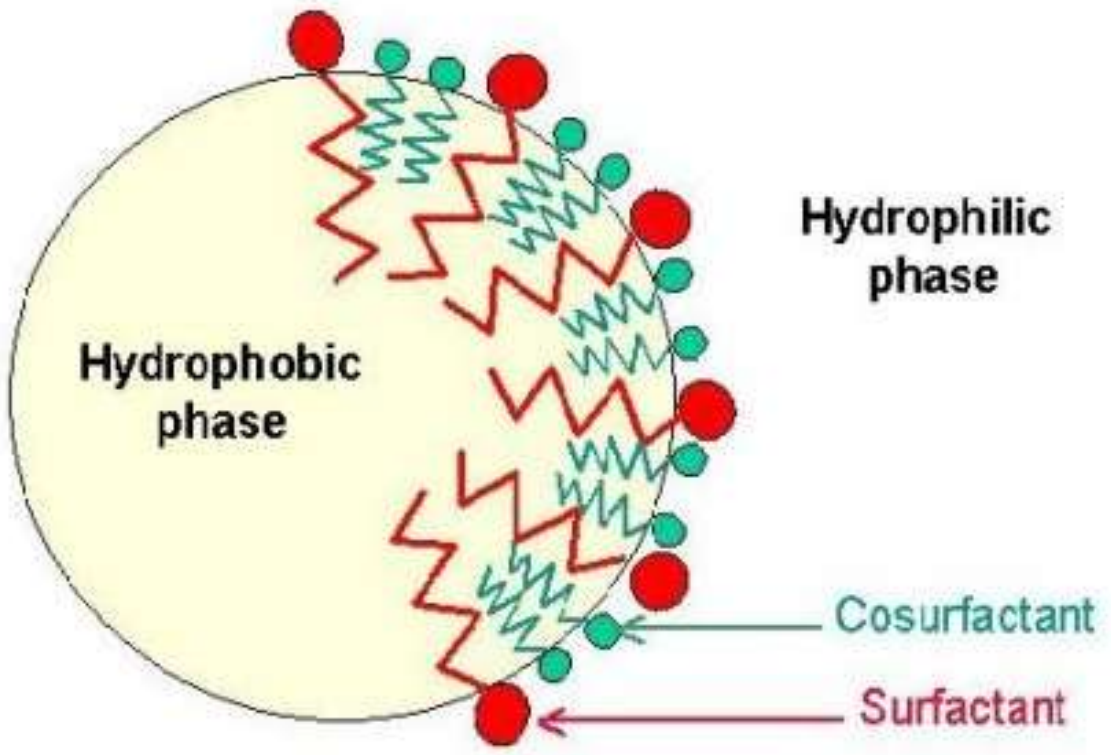

Fig. 2.3. Schemetic diagram of micro-emulsion composed of hydrophobic phase, hydrophilic phase, surfactant, and cosurfactant.

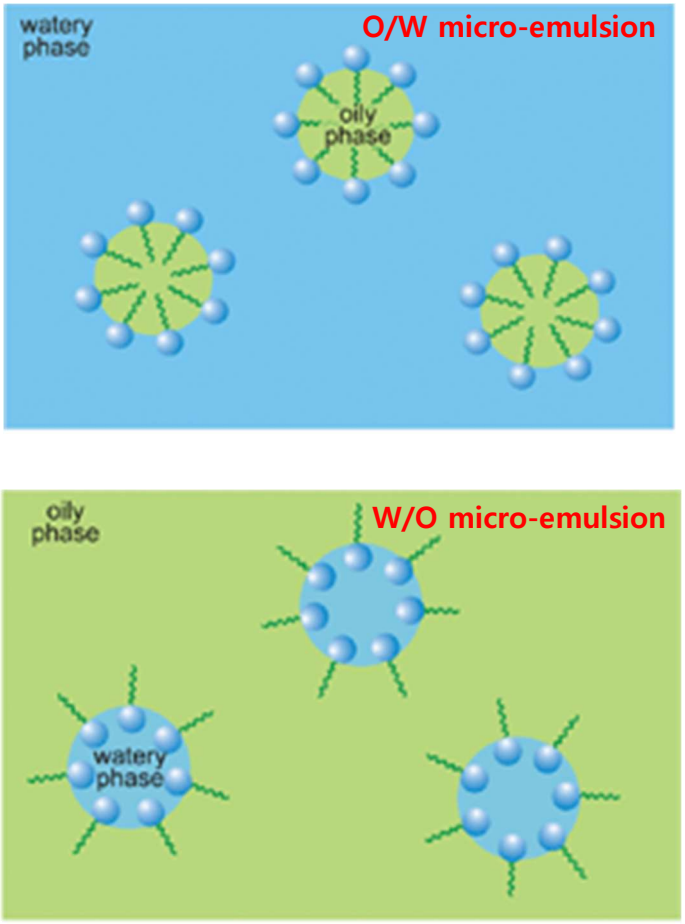

Fig. 2.4. Two kinds of micro-emulsions, oil-in-water (O/W) micro-emulsion and water-in-oil (W/O) micro-emulsion, by the volume ratio between aqueous phase and oily phase.

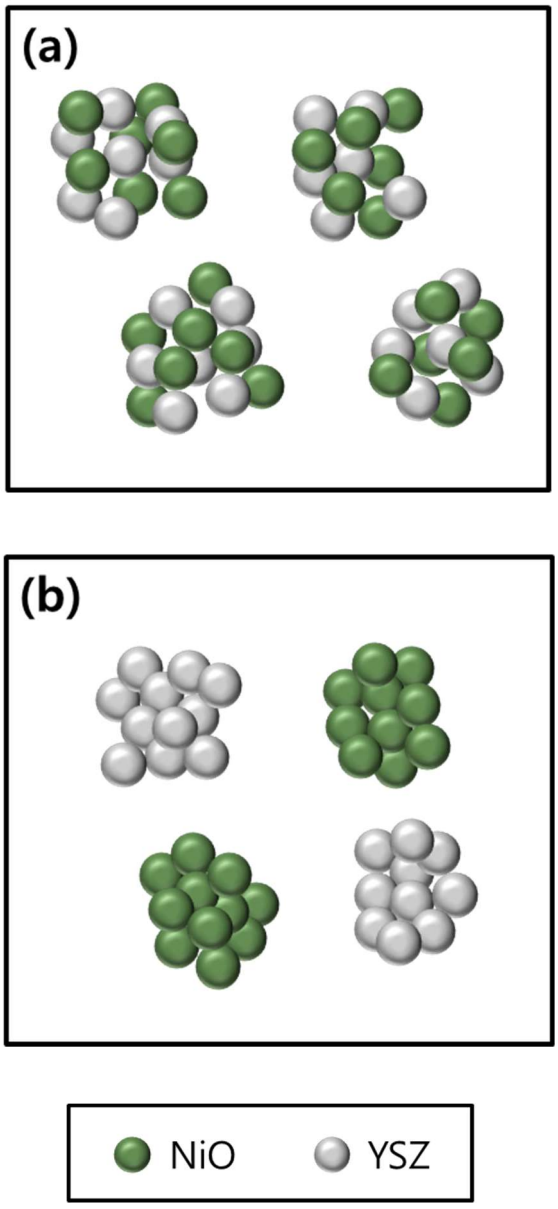

Fig. 2.5. Schemetic diagrams of micro-emulsion synthesized NiO-YSZ powders composed of uniformly distributed NiO and YSZ nano-grains (a), and conventional NiO-YSZ powders composed of uniformly distributed NiO and YSZ nano-particles (b).

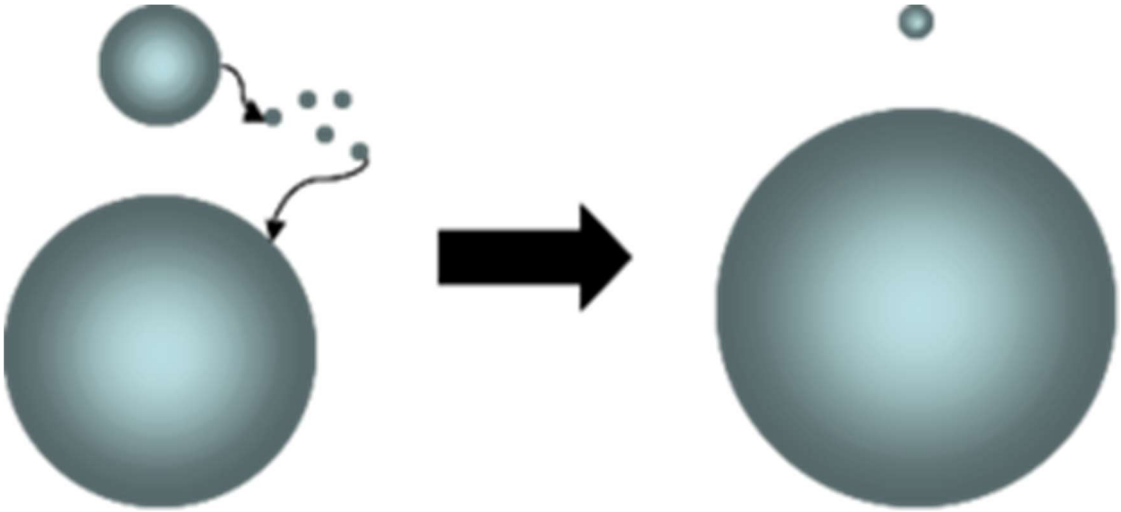

Fig. 2.6. Schemetic diagram of ‘Ostwald ripening’ procedure.

3. Experimental Procedures

3.1 Synthesis of NiO-YSZ nanocomposite powders

NiO-YSZ nanocomposite powders were synthesized by water-in-oil (W/O) micro-emulsion method as shown in **Fig. 3.1**. 100 ml of cyclohexane (C_6H_{12}, Samchun chemicals) was mixed with 12ml Triton X-100 ($C_{14}H_{22}O(C_2H_4O)_n$, Alfa-Aesar) and 10ml pentanol ($C_5H_{12}O$, Alfa-Aesar) to prepare transparent oil phase (O). De-ionized water was used to prepare two types of aqueous phases (A), salt solution and alkali solution, with the compositions mentioned in **Table 3.1**. $Ni(COOCH_3)_2 \cdot 4H_2O$, $Y(NO_3)_3 \cdot 6H_2O$, and $ZrO(NO_3)_2 \cdot 6H_2O$ were dissolved in DI water to fabricate salt solution, and NH_4OH (Alfa-Aesar) was mixed with DI water to prepare alkali solution, respectively. 20ml of salt solution and alkali solution were added slowly into the oil phases to prepare Ni-YSZ micro-emulsion and NH_4OH micro-emulsion, respectively. Ni-YSZ micro-emulsion and NH_4OH micro-emulsion were stirred for 2 hours. Then, two micro-emulsions were mixed and stirred for 12 hours at room temperature for nucleation. The mixture was heated at 80°C for preparing unstable state of micro-emulsion. The precipitates were filtered by aceton and then dried in an oven at 80°C for 12 hours. The dried precipitates were calcined at 500°C for 2 hours with a heating rate of 5°C/min, to synthesize final NiO-YSZ nanocomposite powders.

Conventional NiO-YSZ powders were prepared by mechanical mixing using ball milling process for comparison with micro-emulsion synthesized NiO-YSZ powders. NiO powders (Kceracell) and YSZ powders (TZ-8Y, Tosoh) were taken in a caped Teflon beaker with ethanol and Zr-ball. The ball milling was carried out for 48 hours, then the slurry were dried in oven at 120°C for 12 hours.

3 kinds of NiO-YSZ nanocomposite powders were synthesized by W/O micro-emulsion method with changing the concentrations of alkali solutions during micro-emulsion procedures. Cyclohexane (C_6H_{12}, Samchun chemicals), Triton X-100 ($C_{14}H_{22}O(C_2H_4O)_n$, Alfa-Aesar), pentanol ($C_5H_{12}O$, Alfa-Aesar), $Ni(COOCH_3)_2 \cdot 4H_2O$, $Y(NO_3)_3 \cdot 6H_2O$, $ZrO(NO_3)_2 \cdot 6H_2O$, NH_4OH (Alfa-Aesar), aceton (Samchun

chemicals) were used as the starting materials for micro-emulsion. By changing the volume ratio between DI water (W) and NH_4OH (N) (W:N=0:20, 5:15, 10:10), as shown in **Table 3.2**, 3 types of alkali solutions were prepared, and the final powders from each alkali solutions were named as W0N20, W5N15, and W10N10, respectively.

3.2 Fabrication of an electrolyte-supported single cell

Electrolyte-supported single cells were fabricated to evaluate electrochemical performances. Dense YSZ electrolytes (25Φ, thickness=350μm) were prepared by uniaxial pressing, followed by sintering at 1500ºC for 5 hours. Two types of anode inks were prepared by mechanical mixing of powders (conventional, micro-emulsion) and ESL. Then, the anode inks were brush coated (blade), on the one side of YSZ electrolytes, followed by sintering at 1350ºC for 2 hours. Finally, the LSM-YSZ cathodes [50/50vol/vol. synthesized by conventional mixing of LSM (Fuel Cell Materials) and YSZ(Tosho)] ink were prepared with same process as above. The LSM-YSZ inks were coated on the other side of YSZ electrolytes and sintered at 1100ºC for 2 hours.

Moreover, three types of electrolyte-supported single cells were prepared by using W0N20, W5N15, W10N10 anode powders for electrochemical performance tests, on the purpose of confirming the effects of alkali solution concentrations. The experimental procedures to fabricate electrolyte-supported single cells are same as the methods mentioned above.

3.3 Characterizations and electrochemical performance tests

The crystal phases and crystallinity of the conventional NiO-YSZ powders and the as synthesized micro-emulsion NiO-YSZ powders were analyzed by X-ray diffraction (XRD, Rigaku) with Cu-Kα radiation (λ=0.1542 nm). The thermal decomposition of the dry residue was verified by thermo-gravimetric analysis (TGA) in the temperature range 30-800 ºC with heating rate of 10 ºC/min under continuous flow of 100sccm air. The specific surface area (SSA) of the conventional powders and NiO-

YSZ (μE) powders calcined at 500^0C were confirmed by the BET method (Brunauer–Emmett–Teller). The morphologies of the powder were analyzed by transmission electron microscopy (TEM) and the microstructures of the single cells after cell test were examined by scanning electron microscopy (SEM, Phenom).

Electrolyte-supported single cells were used for electrochemical performance tests. The cells were fixed on the alumina tubes using ceramic bond (Ceramabond™, Aremco product. inc.,), for gas sealing. Silver mesh, Pt-wires and Pt paste were used as current collectors for both anode and cathode. The I-V measurements of single cells were performed at the temperature of 850 °C under continuously supply of 200 cm^3/min humidified (3% H_2O) hydrogen and dry air on anode and cathode sides, respectively. The impedance analysis was also conducted by two-point probe method using a potentiostat (Bio-Logic, VMP-300) with an a perturbation of AC voltage amplitude of 50 mV over the frequency range of 1 MHz to 100 mHz during the fuel operating condition as above.

Phase compositions of three types of powders, W0N20, W5N15, and W10N10, were verified by X-ray diffraction (XRD, Rigaku) with Cu-Kα radiation (λ=0.1542nm). The specific surface areas (SSAs) of the three powders were measured by the BET method. Morphologies of the synthesized powders and cross-sectional images of the single cells were confirmed by transmission electron microscopy (TEM) and scanning electron microscopy (SEM, Phenom), respectively.

3 types of electrolyte-supported single cells which were fabricated by different NiO-YSZ powders (W0N20, W5N15, and W10N10) were employed for cell performance tests. The experimental conditions for I-V measurements and impedance analysis were same with the conditions mentioned above.

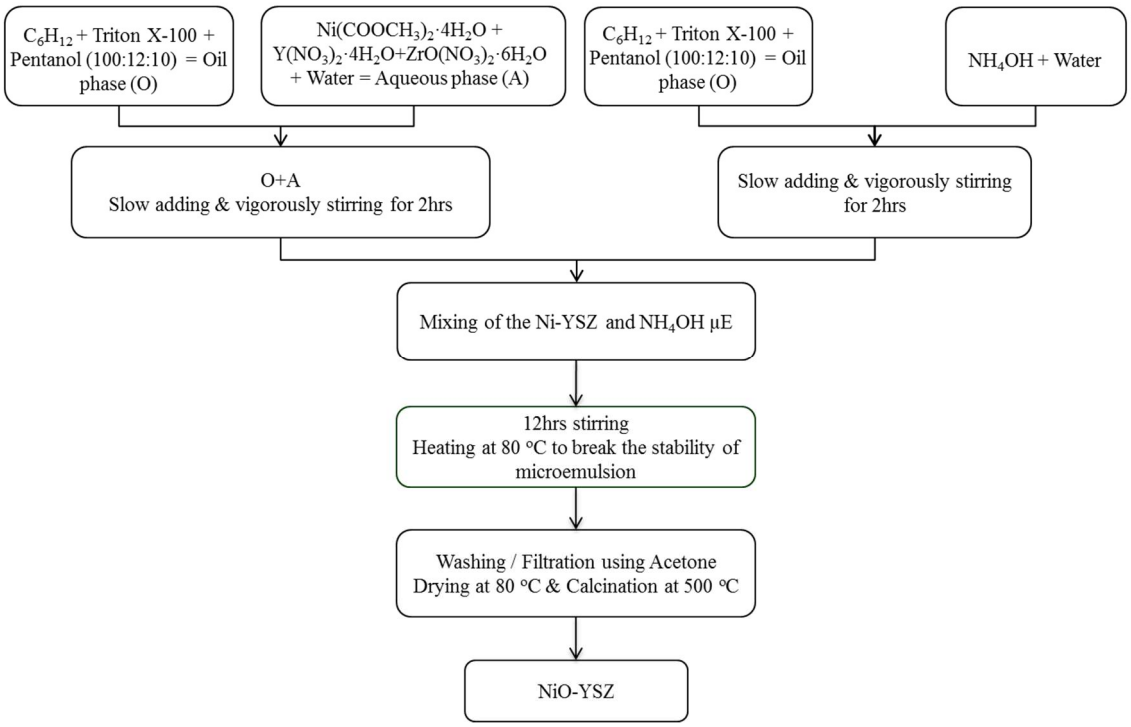

Fig. 3.1. Experimental procedures to synthesize NiO-YSZ powders by micro-emulsion.

Table 3.1. Compositions of salt solution and alkali solution.

	Oil phase	Surfactant		Aqueous phase
	Cyclohexane	Triton X-100	Pentanol	Aqueous solution
Salt solution (ml)	100	12	10	20
Alkali solution (ml)	100	12	10	20

Table 3.2. Compositions of aqueous solution in alkali solution with different kinds of micro-emulsion synthesized NiO-YSZ powders, W10N10, W5N15, and W0N20.

	H_2O	NH_4OH
W10N10 (ml)	10	10
W5N15 (ml)	5	15
W0N20 (ml)	0	20

4. Preparation and Characterization of Ni-YSZ Nanocomposite Anode for Solid Oxide Fuel Cells by Water-in-Oil Micro-emulsion Method

4.1 Introduction

Solid oxide fuel cell (SOFC), which directly converts chemical energy into electrical energy, has high energy efficiency and fuel flexibility, and therefore, it is considered as one of promising technology for energy conversion/power generation [1]. SOFCs have other strengths such as low noise and low greenhouse emission, also [2].

One of the research trends of SOFC is enhancing the electrochemical performance of it. Enhancement of the performance of SOFCs is possible by developing new SOFC materials [3, 4, 6], reducing thickness of the electrolyte [5], and optimizing microstructures and materials of the electrode [6, 7, 8].

Nickel-yttria stabilized zirconia (Ni-YSZ) is the most widely used anode material for SOFCs because of high catalytic activity, mechanical stability, and long-term reliability, etc. [1]. Ni is the catalyst for hydrogen oxidation reaction, and the phase for electron conducting [9]. And YSZ acts as the ionic (oxygen ion) conducting phase [10]. The electrochemical reaction of anode is occurred around the triple-phase boundaries (TPBs) where the ionic conducting phase, electron conducting phase, and gas phase contact. Increment of TPB length enhances the electrochemical performances of anodes [11], and to achieve the enlarged TPB length, initial powder morphologies such as particle size and distribution of components, and microstructure of anode which has fine structure and well distributed phases, are important [12, 13, 14, 15].

NiO-YSZ powders could be obtained by the mechanical mixing, conventionally, however, inhomogeneity and large particle size of NiO and YSZ were observed by this method. To synthesize nano-sized and homogeneously distributed particles, various fabrication methods have been applied: co-precipitation [17, 18], sol-gel [19], gel combustion [20], hydrothermal methods [21], polymeric

complexing [22] and micro-emulsion [16]. Among these methods, the micro-emulsion procedure is a unique technique because it has thermodynamic stability which makes it possible to obtain formation stability. And micro-emulsion methods can be applied by using low-energy equipment, also [23]. NiO-YSZ powders were synthesized by applying water-in-oil (W/O) micro-emulsion methods, here. Effects of micro-emulsion on the properties such as anode morphologies and electrochemical performances were discussed in detail.

4.2 Results and discussion

4.2.1 Phase diagram of micro-emulsion method

The micro-emulsion is a thermodynamically stable liquid mixture of aqueous phase, oil phase, and surfactant. A phase diagram for micro-emulsion method, composed of cyclohexane (oil), Triton X-100+pentanol (surfactant), H_2O (aqueous), is considered to obtain stable W/O micro-emulsion. Phase diagram of micro-emulsion method in **Fig. 4.1.** shows the volume ratio of cyclohexane, Triton X-100+pentanol, and H_2O is 100:22:20. The volume of cyclohexane, Triton X-100, and pentanol was 100:12:10 to obtain transparent oil phases [16].

4.2.2 Thermo-gravimetric analysis

TGA curves of micro-emulsion synthesized NiO-YSZ residues are shown in **Fig. 4.2**. Two significant mass losses are observed in the plots. The weight loss was due to the loss of water and organic components, and decomposition, and the total weight loss was 43.38 %. The temperature of 500 ^oC, which shows a saturation of weight loss, was used as the calcination temperature to obtain pure NiO-YSZ powders.

4.2.3 Phase analysis

XRD patterns of micro-emulsion synthesized NiO-YSZ powders with changing the calcination temperatures are shown in **Fig. 4.3**. All XRD peaks are matched with cubic NiO (Fm3m) and cubic YSZ (Fm3m), and there is no secondary phase. Small peaks of YSZ appear for the powders which were calcined above 500°C, because crystallization of YSZ began at 500°C. This result is consistent with the TGA analysis which shows the saturation of weight above 500°C. XRD peaks of NiO and YSZ become sharper with the increment of calcination temperature, indicating the average crystallite sizes of NiO and YSZ were grown as the calcination temperatures increased. **Fig. 4.4.** and **Table 4.1** show the tendency between the average crystallites sizes calculated by Scherrer equation and the calcination temperature, also. The calculated values of average crystallite sizes for NiO and YSZ at the calcination temperature of 500°C are 14.02 nm and 7.20 nm, respectively. These values show some differences with the sizes of NiO and YSZ from the conventional powders, 42.26 nm and 37.06 nm.

XRD pattern of micro-emulsion synthesized NiO-YSZ powders calcined at 500 °C is compared with that of conventional NiO-YSZ powders, as shown in **Fig. 4.5**. All XRD peaks show good agreement with cubic NiO (Fm3m) and cubic YSZ (Fm3m), without impurity phase. XRD peaks of conventional NiO-YSZ powders are much sharper than those of NiO-YSZ (μE) powders, which indicates powders which have smaller crystallite sizes can be obtained by applying micro-emulsion procedures.

4.2.4 Morphology analysis

TEM images of conventional powders and micro-emulsion synthesized powders are shown in **Fig. 4.6**. The particle sizes of micro-emulsion prepared powders are smaller than those of conventional powders, obviously. However, the dispersities of both powders seem like indifferent.

The particle size distributions of two types of powders from the TEM images are shown in **Fig. 4.7**, and the average particle sizes are 40.20 nm and 90.27 nm, in the case of micro-emulsion synthesized NiO-YSZ and conventional NiO-YSZ, respectively. Moreover, particles obtained by micro-emulsion show much narrow distribution than conventional particles.

The measured specific surface area (SSA) values of conventional powders and micro-emulsion synthesized powders are 6.164 m^2/g and 14.976 m^2/g, respectively. Equivalent diameters of the powders can be calculated by the equation:

$D_{BET} = 6/(\rho \times S_{BET})$,

where D_{BET} is the equivalent diameters of the particles, S_{BET} is the specific surface area of the particles, and ρ is the theoretical density. The calculated equivalent diameters of conventional powders and micro-emulsion prepared powders are 154.888 nm and 63.744 nm, respectively. These calculated values are a little different with the observed sizes from TEM images as shown in **Table 4.2**, which might be caused by the existence of some agglomerations.

TEM mapping images of conventional NiO-YSZ powders and micro-emulsion synthesized NiO-YSZ powders are shown in **Fig. 4.8**, indicating well distribution of atomic elements, Ni, Y, Zr, in the both cases.

Cross-sectional images of electrolyte-supported single cells after cell tests are shown in **Fig. 4.10**. Porous structures of Ni-YSZ anodes are shown in both cases, that is, the cross-section of conventional cell and micro-emulsion prepared cell. However, the grain size of micro-emulsion fabricated cell is much smaller than that of conventional cell.

4.2.5 Electrochemical performance

The I-V and the I-P curves of single cells composed of conventional Ni-YSZ anode and micro-emulsion prepared Ni-YSZ anode at the operating temperature of 850 ^oC are shown in **Fig. 4.9 (a)**. The maximum power density of conventional cell and micro-emulsion fabricated cell are 203.84 mW/cm^2 and 359.033 mW/cm^2, respectively, and the increment of maximum power density is 76.14 %.

The EIS spectra of conventional cell and micro-emulsion prepared cell at the operating temperature of 850 ^oC are shown in **Fig. 4.9 (b)**. The electrode resistances of single cells are 1.14 $\Omega\ cm^2$ and 0.44 $\Omega\ cm^2$, in the case of conventional cell and micro-emulsion fabricated cell, respectively, and decrease of electrode resistance is 61.49 %.

4.3 Conclusions

Homogeneously distributed NiO-YSZ nanocomposite particles for nanostructured anode were synthesized successfully by water-in-oil micro-emulsion method. The particle size of NiO-YSZ powders synthesized by micro-emulsion, calcined at 500 ^{o}C was around 40 nm. Electrochemical performances were improved by the nanocomposite anode synthesized by micro-emulsion, compared with the results obtained by the conventional anode. A single cell with micro-emulsion synthesized Ni-YSZ anode showed a higher maximum power density, 359 mW cm^{-2}, compared with that of a single cell with conventional Ni-YSZ anode, 204 mW cm^{-2}, at the operating temperature of 850 ^{o}C. The electrode resistance of a single cell decreased to 0.44 Ω cm^2 with micro-emulsion synthesized anode, compared with the value of a conventional cell, 1.14 Ω cm^2, at the same operating temperature with I-V analysis. The electrochemical performance of a single cell was improved by the enlarged TPB obtained by the micro-emulsion synthesized Ni-YSZ anode composed of uniformly distributed nano-grains.

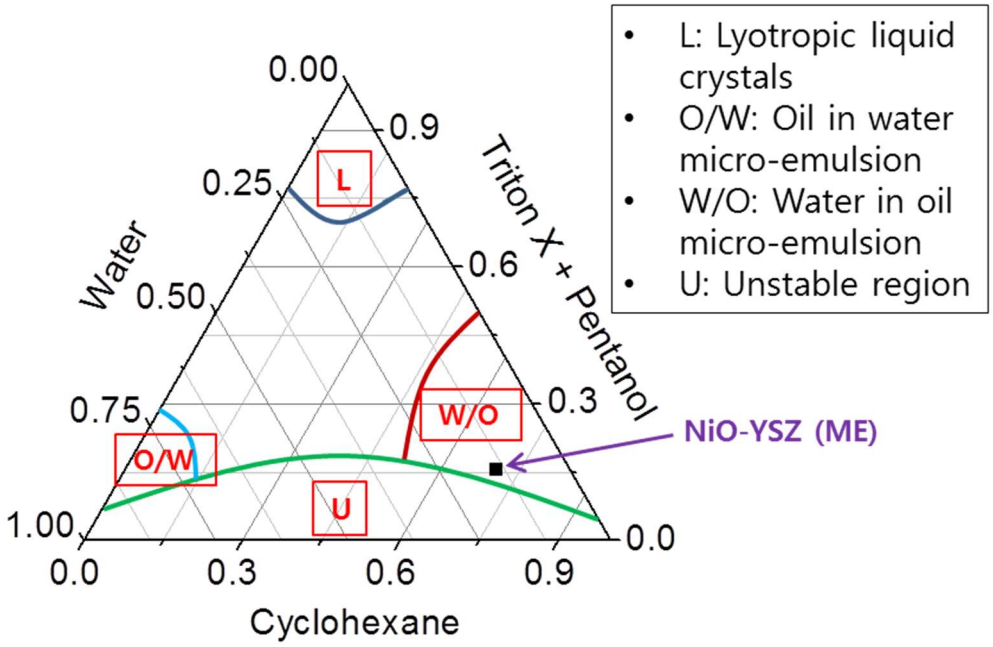

Fig. 4.1. Phase diagram of micro-emulsion procedure to synthesize NiO-YSZ powders.

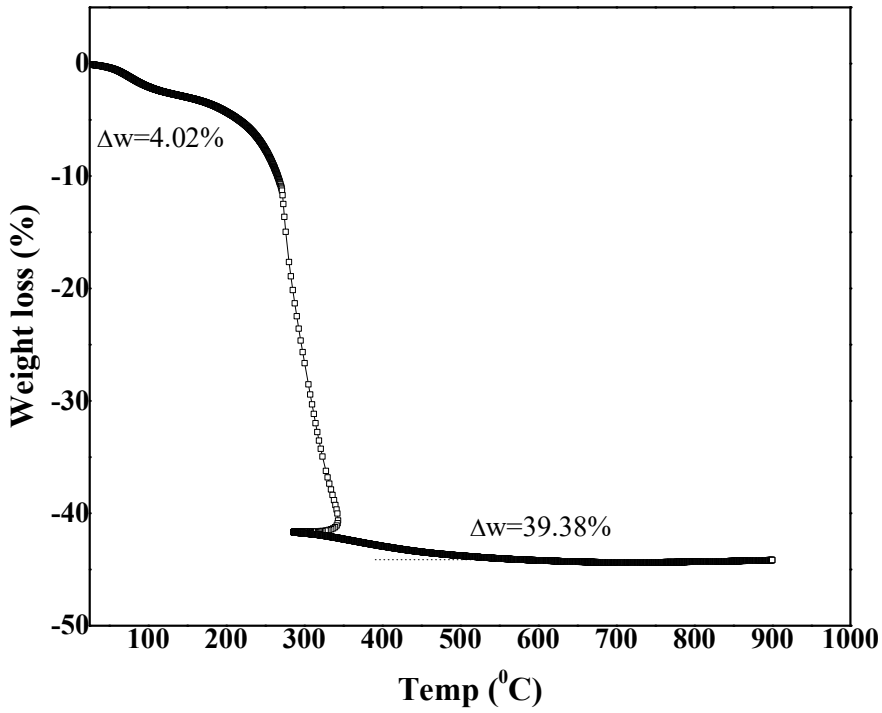

Fig. 4.2. TG curves of the precipitates.

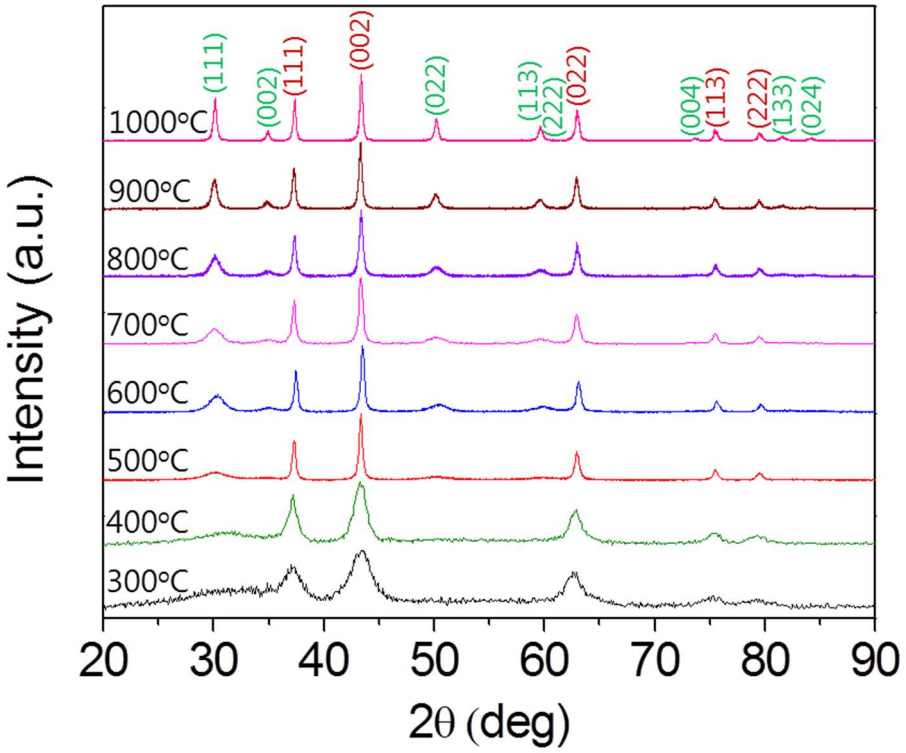

Fig. 4.3. XRD patterns of NiO-YSZ (micro-emulsion) with changing the calcination temperature.

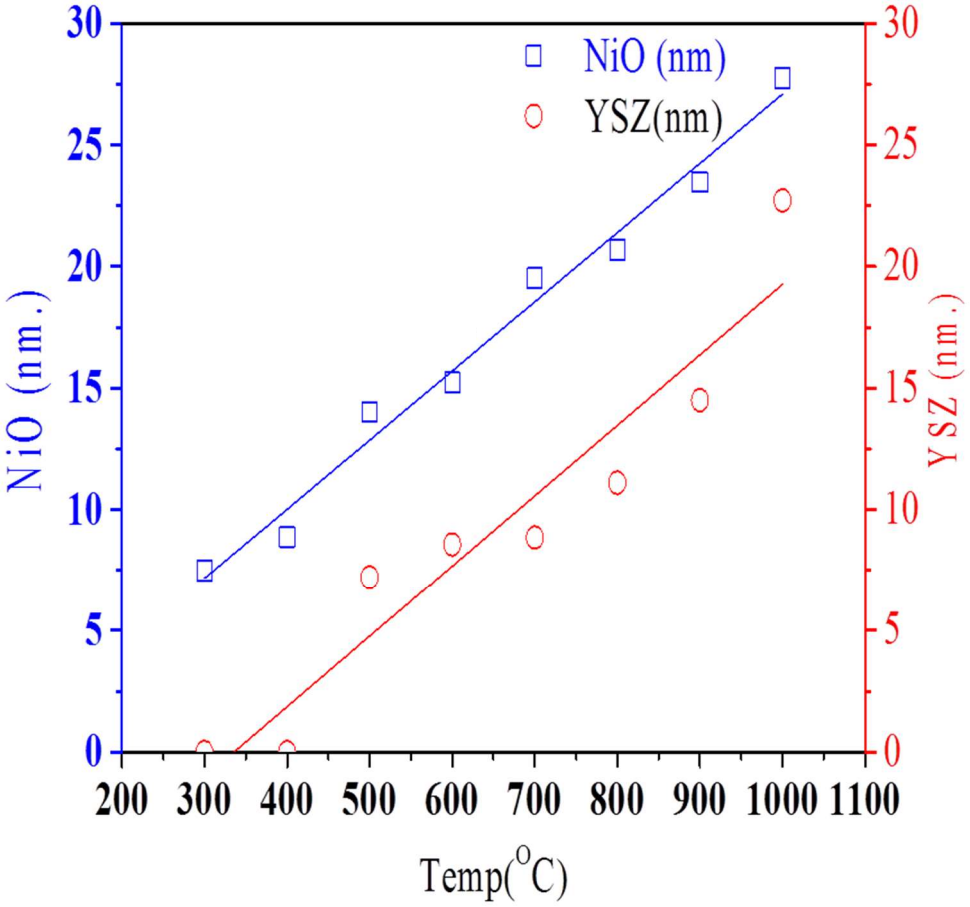

Fig. 4.4. Average crystallites size of NiO-YSZ (micro-emulsion) with changing the calcination temperature.

Table 4.1. Average crystallites sizes of NiO-YSZ (micro-emulsion) powders with changing the calcination temperature, and the size of conventional NiO-YSZ powders.

Temp (^{0}C)	NiO (nm)	YSZ(nm)
300	7.50	-
400	8.88	-
500	**14.02**	**7.20**
600	15.22	8.56
700	19.52	8.85
800	20.70	11.11
900	23.48	14.50
1000	27.75	22.72
Conventional	**42.26**	**37.06**

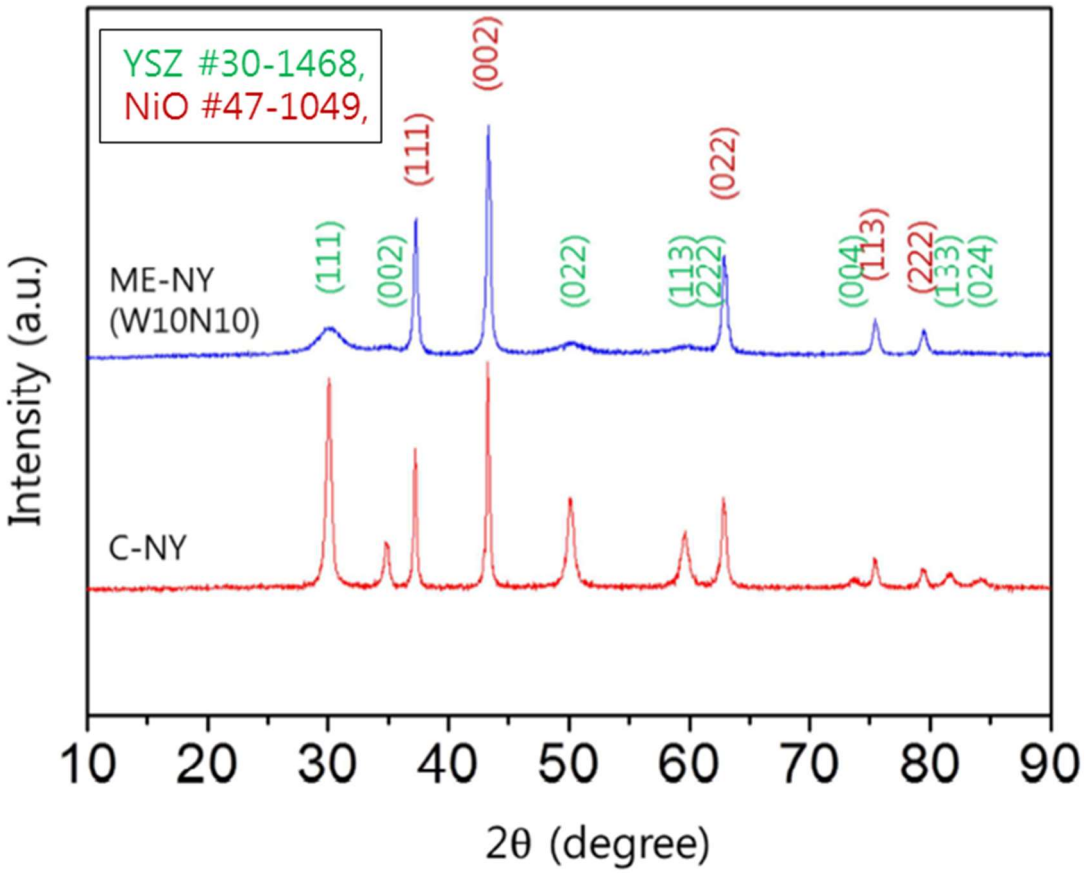

Fig 4.5. XRD patterns of NiO-YSZ (conventional) and NiO-YSZ (micro-emulsion) powders.

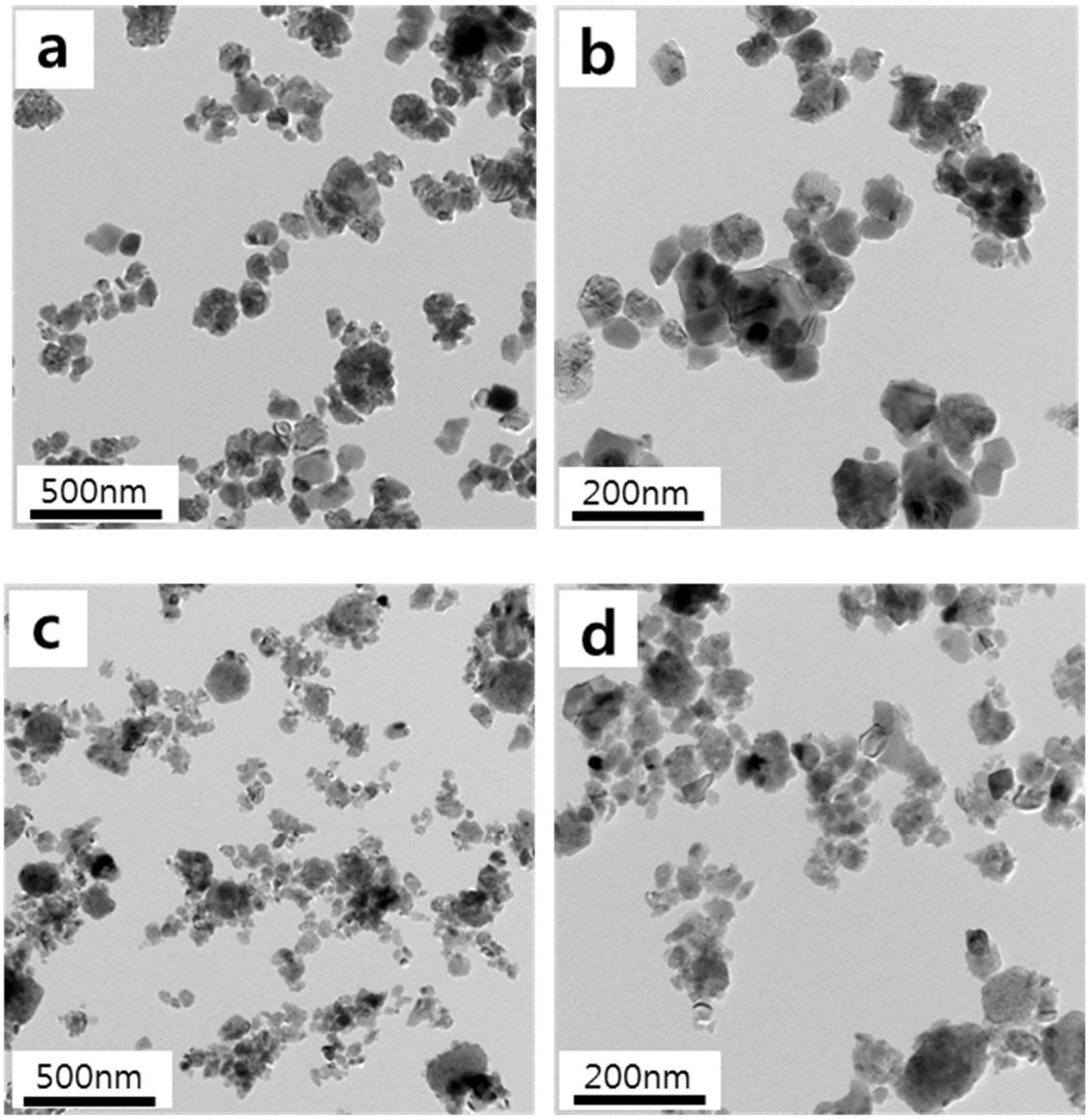

Fig 4.6. TEM images of conventional NiO-YSZ powder (a) and (b); NiO-YSZ (micro-emulsion) powder (c) and (d) calcined at 500 ºC.

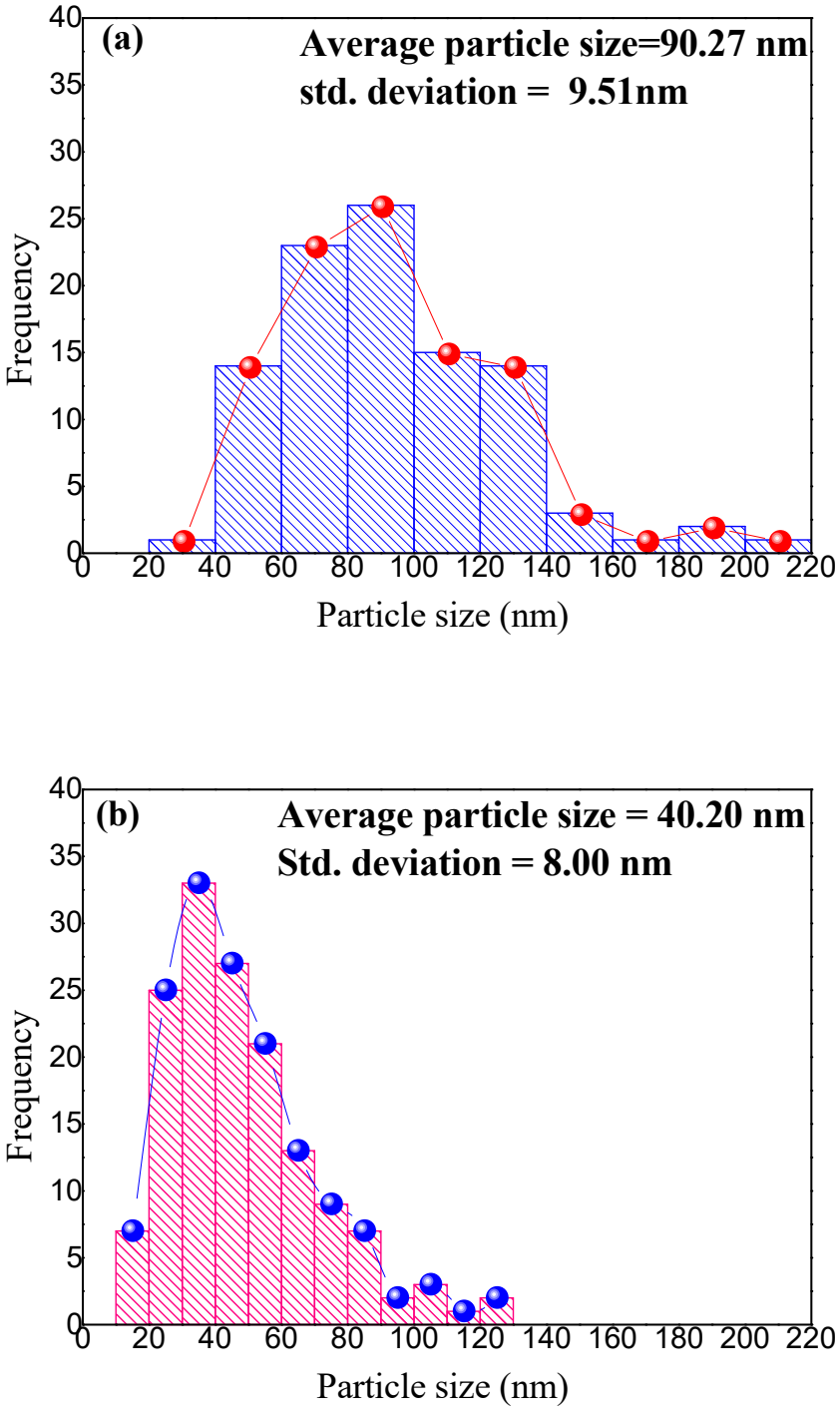

Fig 4.7. Particle size distributions of conventional NiO-YSZ powder (a) and micro-emulsion NiO-YSZ powder (b).

Table 4.2. Crystallites sizes and particle sizes of conventional NiO-YSZ powders and micro-emulsion synthesized NiO-YSZ powders from XRD, TEM, BET.

	Crystallites size (nm)		Particle size (nm)	
	XRD (NiO)	XRD (YSZ)	TEM	BET
Conventional (nm)	31.378	14.242	68.993	154.888
Micro-emulsion (nm)	23.480	3.605	41.500	63.744

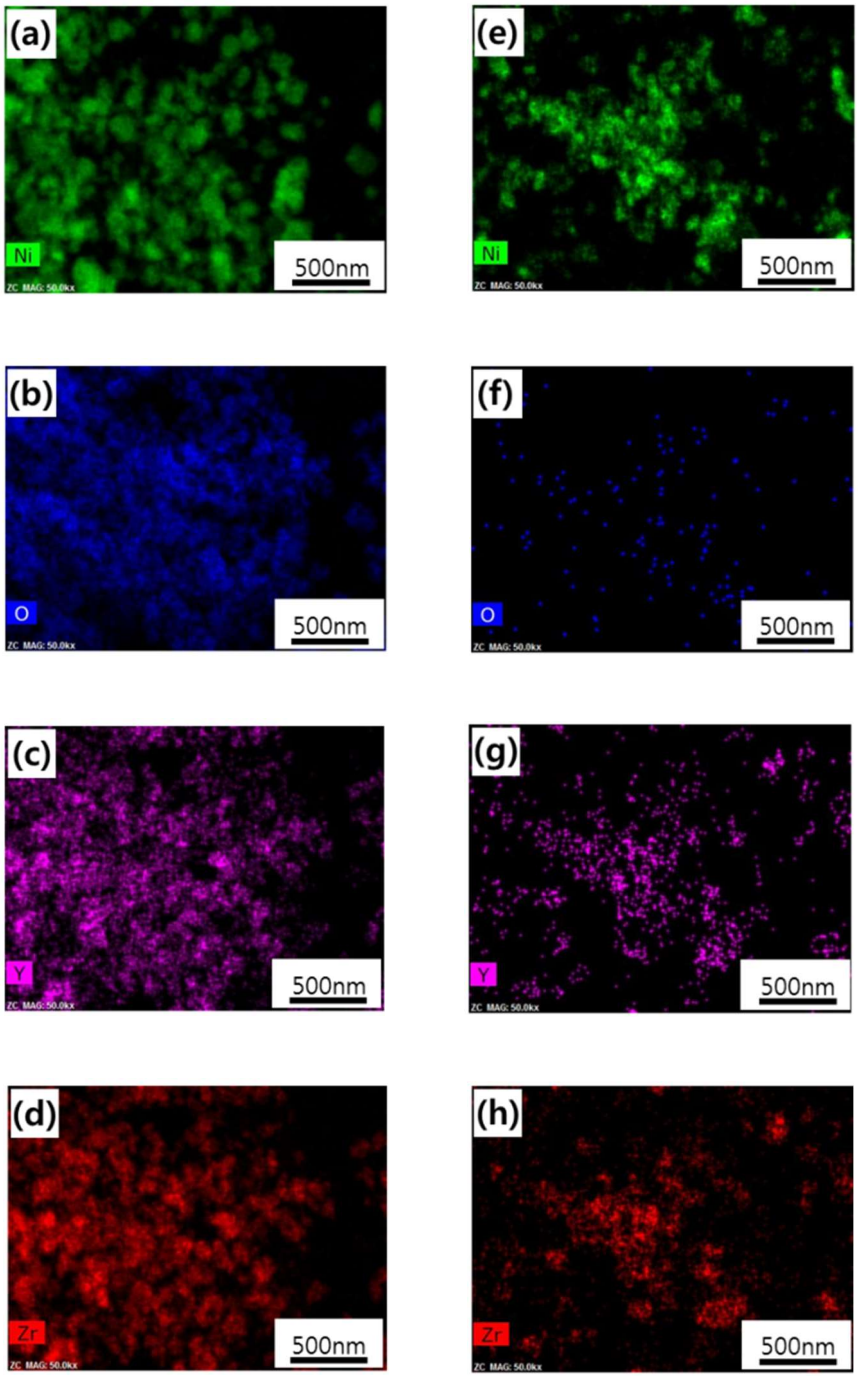

Fig. 4.8. TEM mappings of conventional NiO-YSZ powder (a), (b). (c) and (d); NiO-YSZ (micro-emulsion) powder (e), (f), (g) and (h).

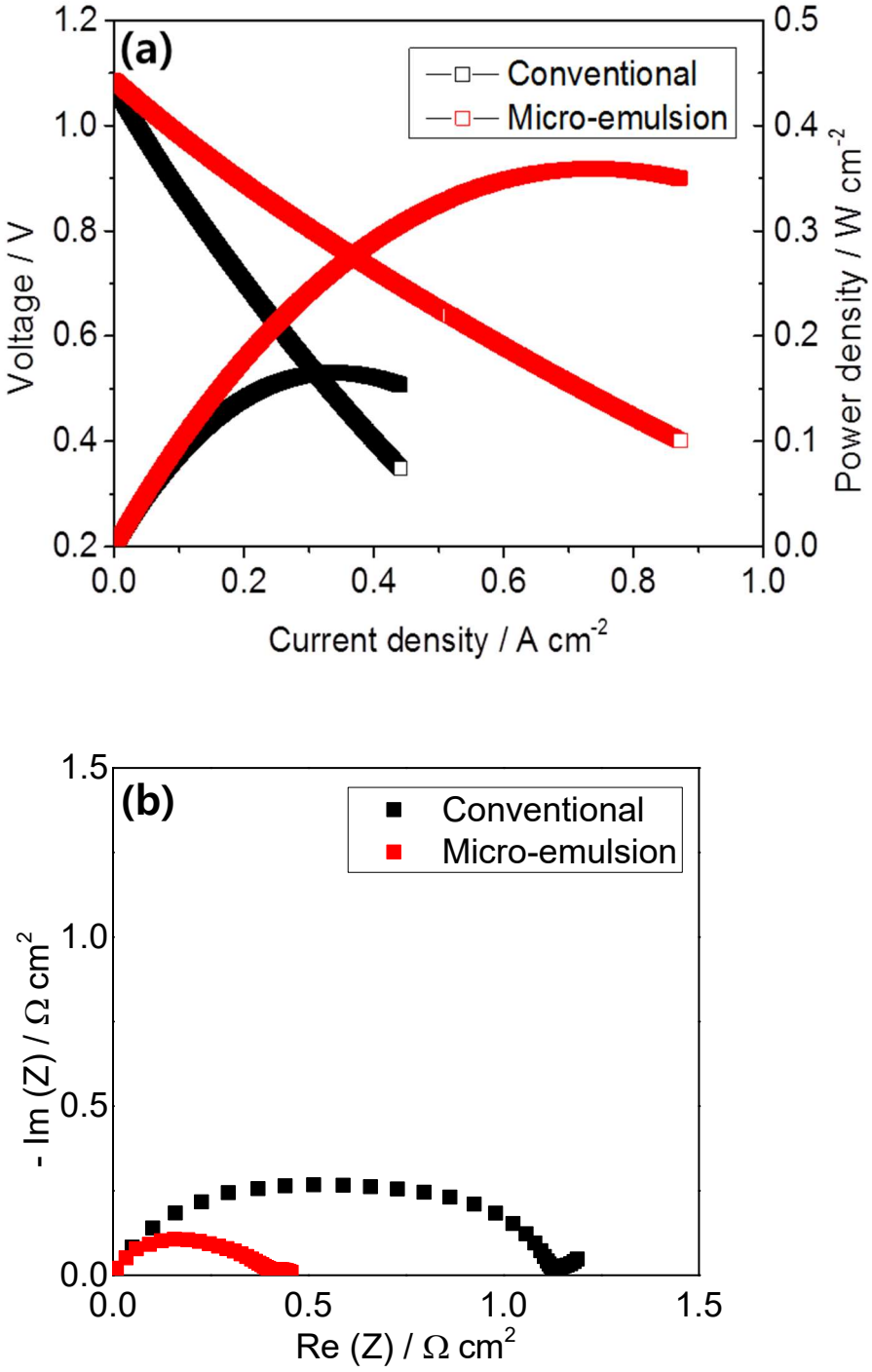

Fig. 4.9. I-V and I-P curves of single cells composed of conventional Ni-YSZ anode and micro-emulsion prepared Ni-YSZ anode (a), and EIS spectra of conventional single cell and micro-emulsion fabricated single cell.

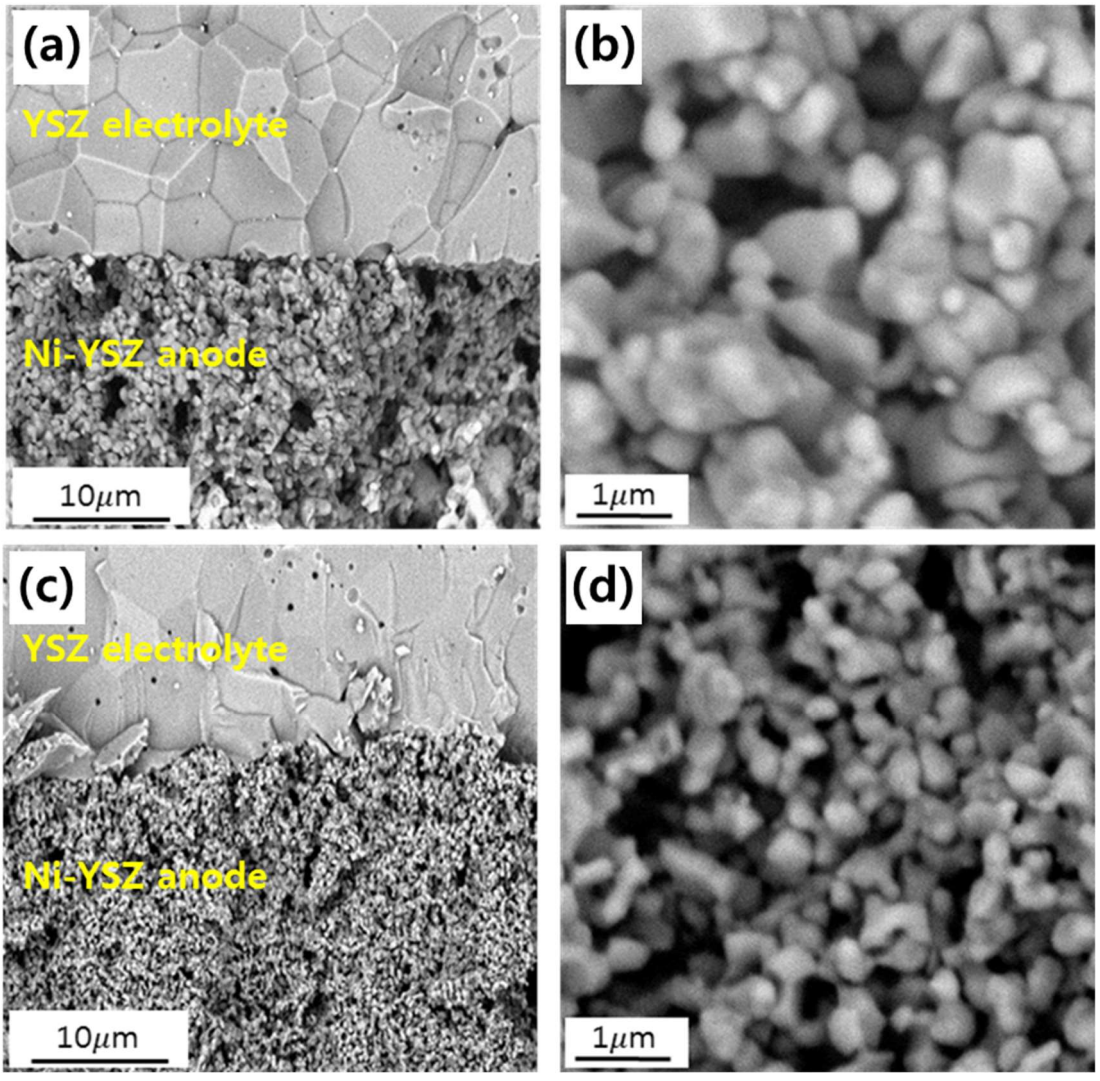

Fig. 4.10. Microstructures of Ni-YSZ anode after electrochemical tests. (a) and (b) SEM images of conventional Ni-YSZ anode. (c) and (d) SEM images of micro-emulsion fabricated Ni-YSZ anode.

5. Effects of Alkali Solution Concentrations on the Properties of Ni-YSZ Nanocomposite Anode Prepared by Water-in-Oil Micro-emulsion Method

5.1 Introduction

Solid oxide fuel cell (SOFC), a solid-state device which directly converts chemical energy into electricity, has attracted many attentions because of fuel flexibility and high energy conversion efficiency [1, 2].

One of the main issues of SOFC is enhancing the electrochemical performance of it. To enhance the performance of SOFCs, several researches related with developing new SOFC materials [3, 4, 6], reducing thickness of the electrolyte [5], and optimizing microstructures and materials of the electrode [6, 7, 8].

Nickel-yttria stabilized zirconia (Ni-YSZ) is a state-of-art material for SOFC anode due to high catalytic activity for hydrogen oxidation reaction (HOR), mechanical stability, and long-term reliability, etc [1]. In the case of Ni-YSZ, Ni and YSZ act as electron conducting phase and ionic (oxygen ion) conducting phase, respectively [9, 10]. Electrochemical reactions of the anode are occurred at the triple-phase boundaries (TPBs) where electron conducting phase, ionic conducting phase, and gas phase meet. The electrochemical performances of the anode can be enhanced by enlargement of the TPBs, and therefore, several researches for increased TPB length have been reported. Controlling of the initial powder morphologies such as distribution of the individual components and particle sizes, and optimizing of the microstructures which have well distributed and fine structures have been studied [12, 13, 14, 15].

Micro-emulsion applied to synthesize NiO-YSZ powders which have nano-sized and homogeneously distributed particles, in our previous studies. It was revealed that micro-emulsion synthesized Ni-YSZ

anode shows improved electrochemical performance, comparing with that of the conventional Ni-YSZ anode. However, the concentration of the alkali solution for precipitation of the particles was not optimized. Alkali solution concentration is adjusted to obtain powders which have improved properties.

5.2 Results and discussion

5.2.1 Phase diagram of micro-emulsion method

The micro-emulsion is a liquid mixture of oil phase, aqueous phase, and surfactant. Phase diagrams for micro-emulsion method are considered to obtain thermodynamically stable W/O micro-emulsion. Phase diagrams of the W/O micro-emulsion composed of cyclohexane (oil), H_2O (aqueous), and Triton X-100 + pentanol (surfactant) with varied alkali solution concentrations are shown in **Fig. 5.1**. Three types of micro-emulsion for synthesizing different NiO-YSZ powders, W10N10, W5N15, and W0N20 have same volume ratio between cyclohexane, Triton X-100+pentanol, and H_2O (100:22:20). To obtain transparent oil phases, volume ratio between cyclohexane, Triton X-100, and pentanol was fixed to 100:12:10. **Fig. 5.1** also shows the phase diagram of micro-emulsion composed of cyclohexane (oil), Triton X-100+pentanol (surfactant), and NH_4OH. Three powders, W10N10, W5N15, and W0N20, which were synthesized by different alkali solution concentrations have distinct positions in the phase diagram.

5.2.2 Phase analysis

XRD patterns of NiO-YSZ (μE) powders synthesized by different alkali solution concentrations are shown in **Fig. 5.2**. All XRD peaks are well matched with cubic NiO (space group: Fm3m) and cubic YSZ (space group: Fm3m), and there is no impurity phase. The average crystallite sizes decrease as the alkali solution concentrations increases, which can be shown in **Fig. 5.3**.

5.2.3 Morphology analysis

Fig. 5.4. shows TEM images of the three powders, W10N10, W5N15, and W0N20. Nanoscale particles are observed in all of the powders, as shown in this figure. The average particle sizes are 40.20 nm, 36.87 nm, and 31.54 nm, respectively, from the particle size distribution diagrams, as shown in **Fig. 5.5**. The average particle sizes decrease as the alkali solution concentrations increase, which has the same tendency with the changes of the crystallite sizes calculated by the Scherrer equation. Moreover, standard deviations of the particle sizes decrease, from W10N10 to W0N20.

The measured specific surface area (SSA) values are 14.976 m^2/g, 34.082 m^2/g, and 42.268 m^2/g, respectively, in the case of W10N10, W5N15, and W0N20. BET equivalent diameters are calculated by the equation:

$$D_{BET} = 6/(\rho \times S_{BET}),$$

where D_{BET} is the equivalent diameter, ρ is the theoretical density, and S_{BET} is the specific surface area of the particles. The calculated equivalent diameters are 63.744 nm, 28.010 nm, and 22.568 nm, respectively. The equivalent diameters decrease from W10N10 to W0N20, with increment of the alkali concentrations. The estimated values of W5N15 and W0N20 are well matched with the particle sizes from TEM images, however, in the case of W10N10, difference between two values is existed, which might be caused by some agglomerations of the powders.

Cross-sectional images of the single cells after electrochemical tests are shown in **Fig. 5.7**. Although the particle sizes of NiO-YSZ (W10N10) and NiO-YSZ (W0N20) show some differences, the cross-sectional microstructures after reduction are very similar. Porous Ni-YSZ anodes are shown in both cases, and the grain sizes are not much different.

5.2.4 Electrochemical performance

The I-V and I-P curves of the single cells composed of Ni-YSZ anode (W10N10) and Ni-YSZ anode (W0N20) are shown in **Fig. 5.6 (a)**. Although the microstructures such as particle sizes of NiO-YSZ

(W10N10) and NiO-YSZ (W0N20) are different, the I-V and I-P curves of two kinds of cells are almost same. However, the electrode resistances of the single cells at the operating temperature 850 ^{o}C and open circuit voltage (OCV) show some differences, as shown in **Fig. 5.6 (b)**. The values of electrode resistances are 0.44 Ω cm^2 and 0.65 Ω cm^2, respectively, in the case of single cells composed of Ni-YSZ anode (W10N10) and Ni-YSZ anode (W0N20). Increment of the electrode resistance at the open circuit potential is 48.17 %.

5.3 Conclusions

Three types of micro-emulsion synthesized NiO-YSZ nanocomposite powders, W10N10, W5N15, and W0N20, with different alkali concentrations, were successfully synthesized. Particle size of W0N20 decreased to 30nm compared with the value of W10N10, around 40nm. Moreover, specific surface area of W0N20 drastically increased to 42.27 m^2/g, from the value of W10N10, 14.98 m^2/g. However, the maximum power density of a single cell was not affected by the alkali concentrations. The electrode resistance of a single cell with W0N20 showed a higher value of 0.65 Ω cm^2, compared with the value of a single cell with W10N10, 0.44 Ω cm^2, at the open circuit voltage with the operating temperature of 850 ^{o}C, although the particle size of W0N20 is smaller than that of W10N10. The reduced TPB length caused by the agglomeration of too small particles might be the reason of the electrochemical performances of single cells.

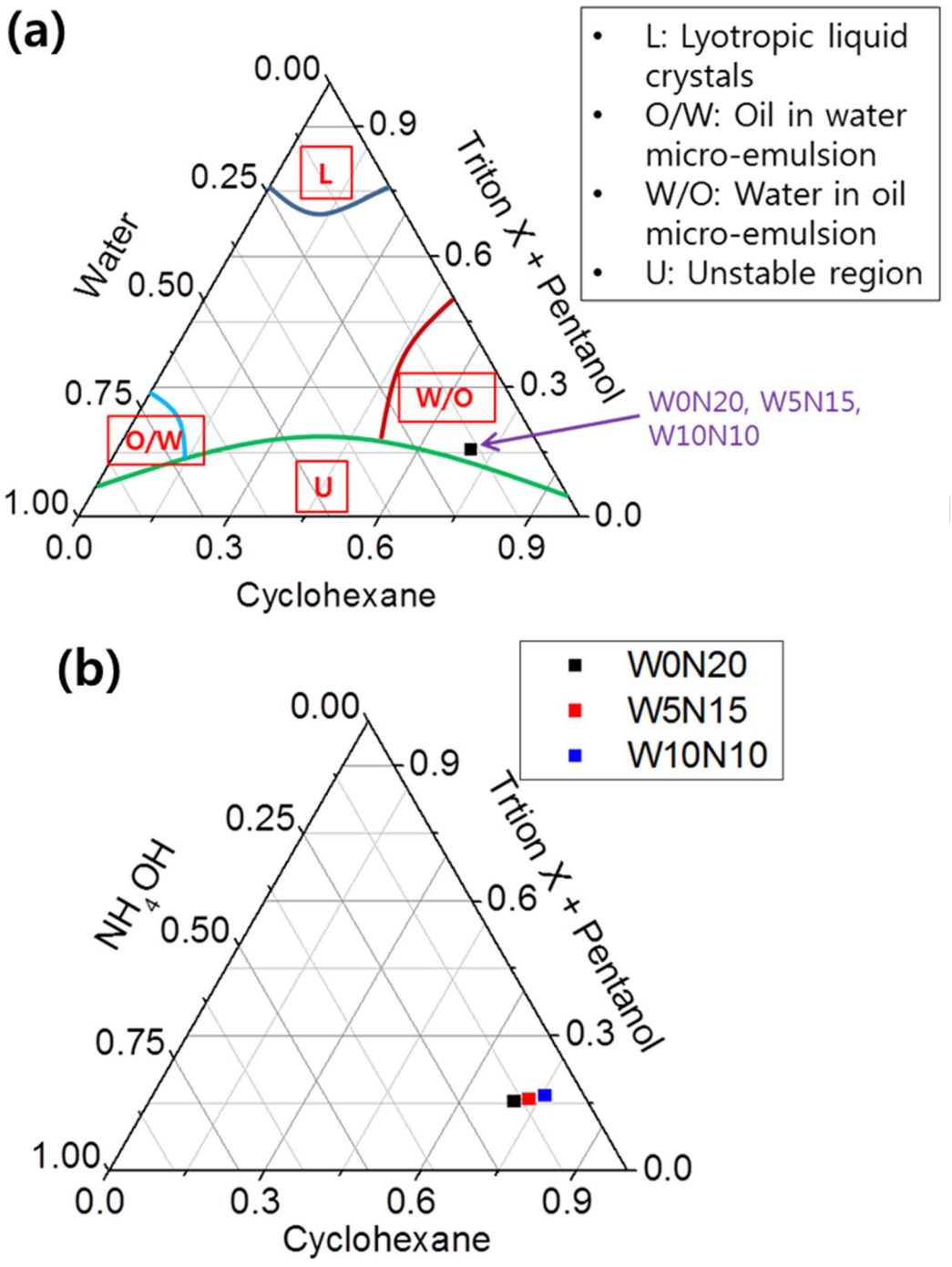

Fig. 5.1. Phase diagrams of micro-emulsion procedure to synthesize NiO-YSZ powders; W0N20, W5N15, and W10N10. (a) Phase diagram composed of cyclohexane, triton X + pentanol, and water. (b) Phase diagram composed of cyclohexane, triton X + pentanol, and NH_4OH.

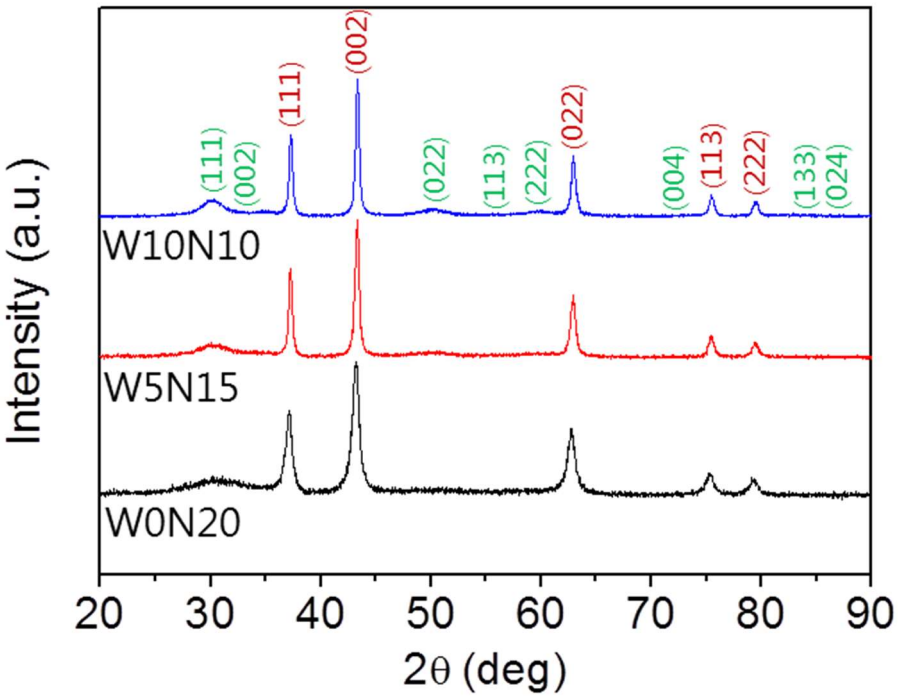

Fig. 5.2. XRD patterns of micro-emulsion synthesized powders (W0N20, W5N15, and W10N10).

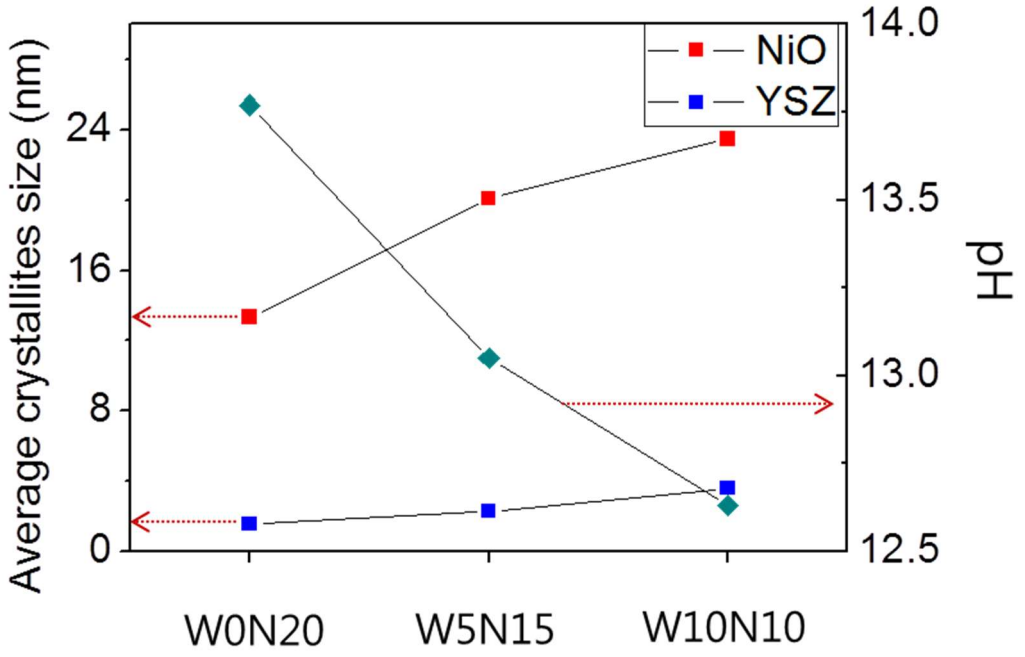

Fig. 5.3. Average crystallites size of micro-emulsion synthesized powders (W0N20, W5N15, and W10N10) with alkali solution pH.

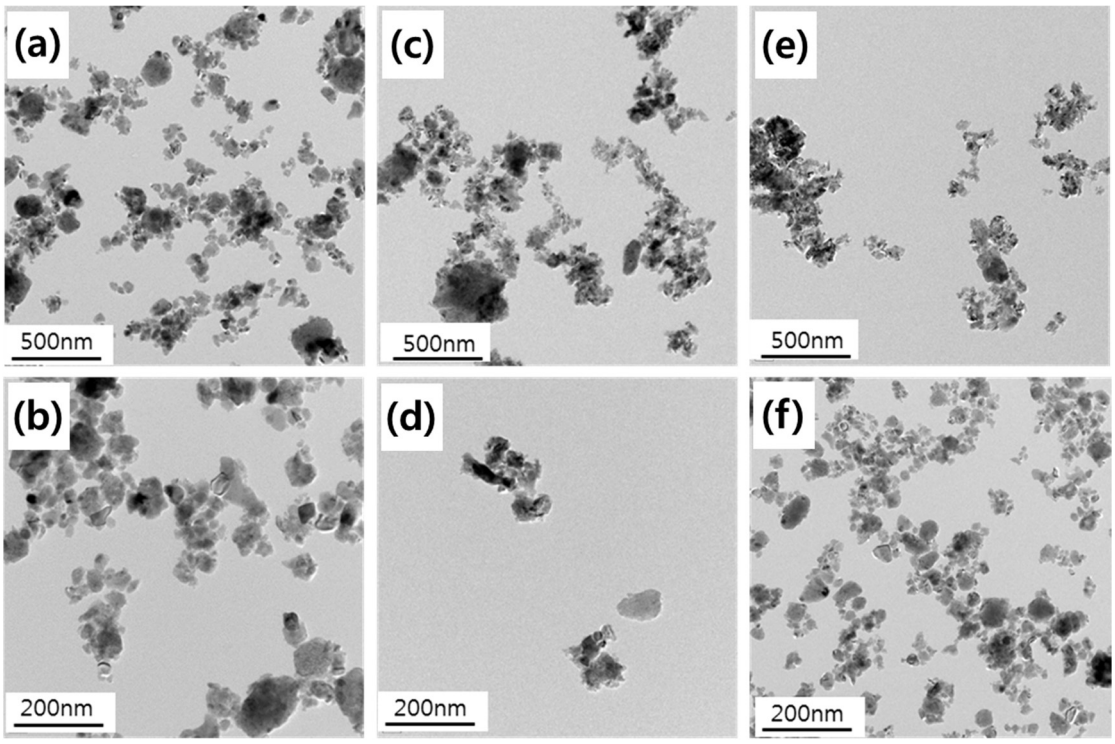

Fig 5.4. TEM images of NiO-YSZ (micro-emulsion) powders prepared by different alkali concentrations. (a) and (b) images of W10N10, (c) and (d) images of W5N15, and (e) and (f) images of W0N20.

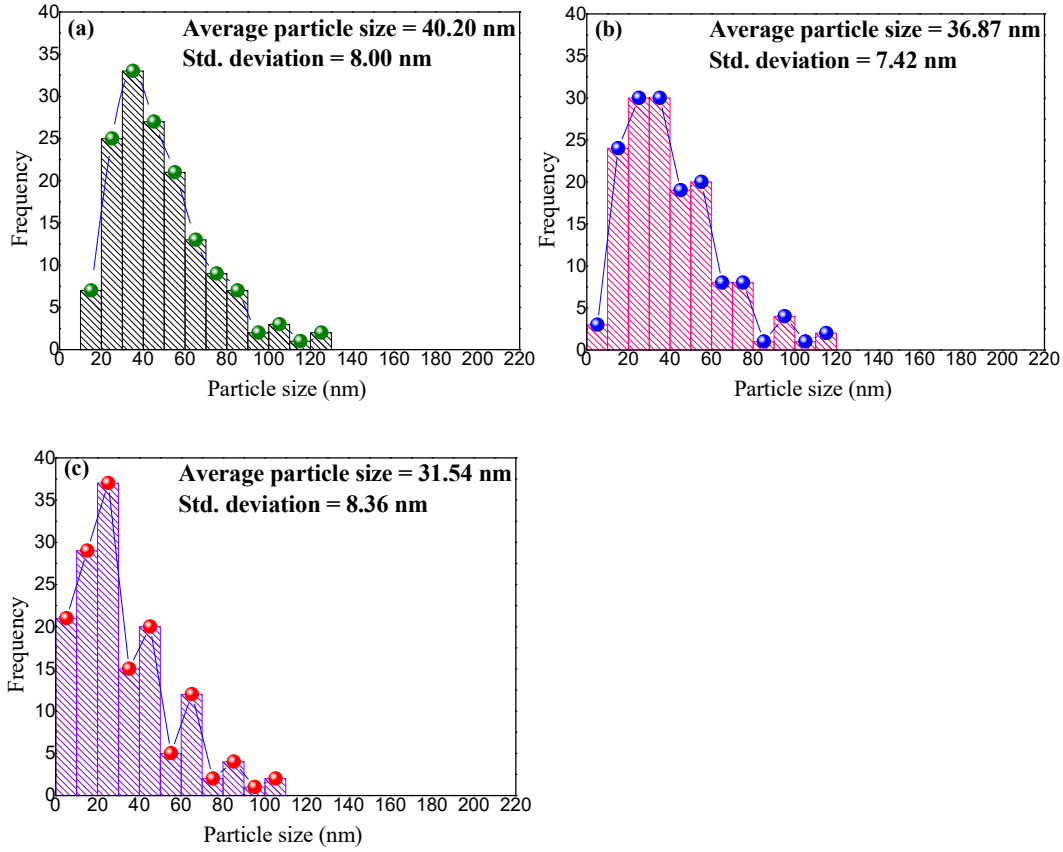

Fig. 5.5. Particle size distributions of NiO-YSZ (micro-emulsion) powders with different alkali concentrations. (a) distributions of W10N10. (b) distributions of W5N15. (c) distributions of W0N20.

Table 5.1. Crystallites sizes and particle sizes of NiO-YSZ (micro-emulsion) powders with different alkali concentrations from XRD, TEM, and BET.

	Crystallites size (nm)		Particle size (nm)	
	XRD (NiO)	XRD (YSZ)	TEM	BET
W10N10 (nm)	23.480	3.605	40.200	63.744
W5N15 (nm)	20.087	2.289	36.870	28.010
W0N20 (nm)	13.347	1.561	31.540	22.568

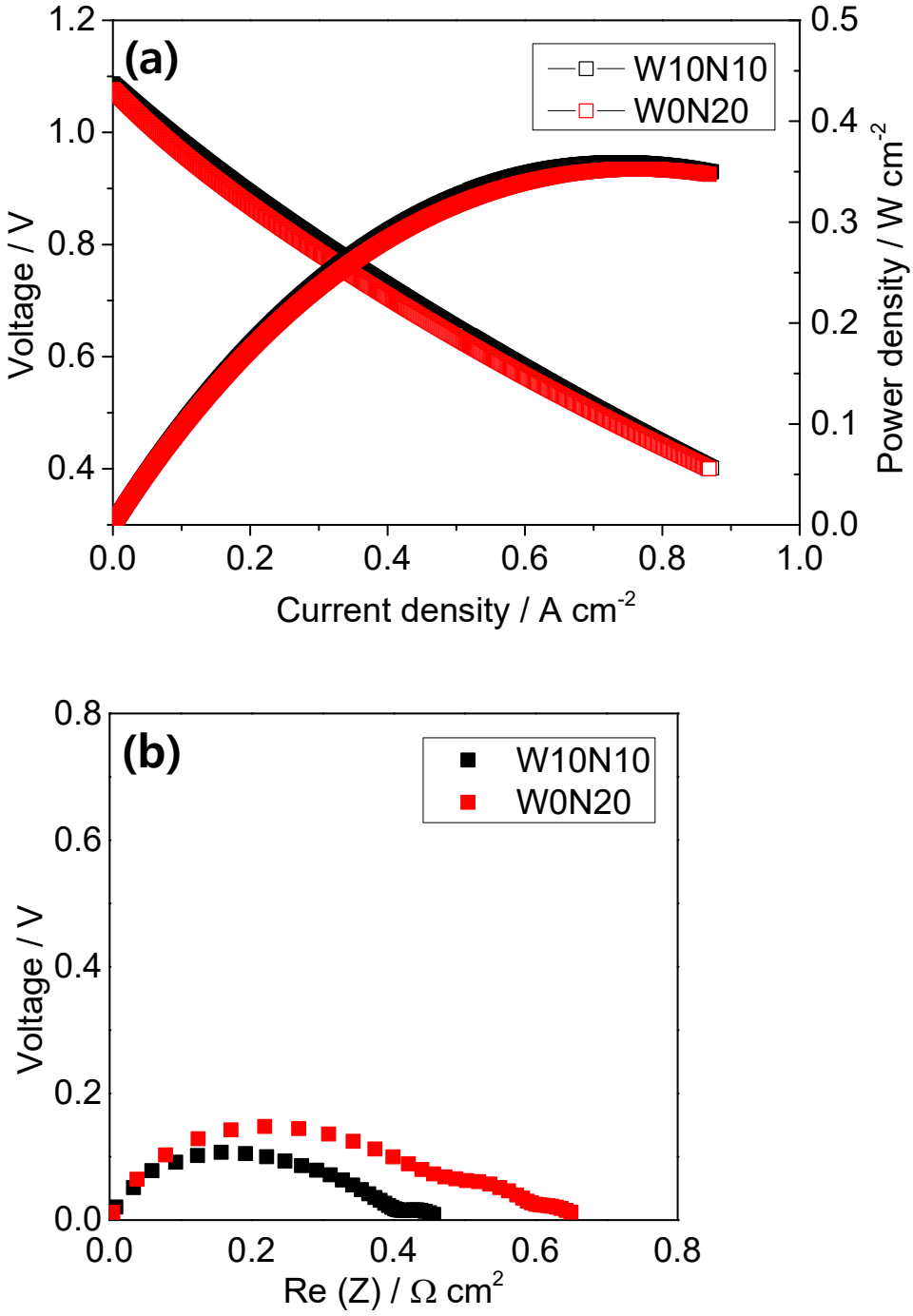

Fig. 5.6. I-V and I-P curves of single cells composed of Ni-YSZ anode fabricated by micro-emulsion with different alkali concentrations (a), and EIS spectra of micro-emulsion fabricated single cells composed of W10N10 and W0N20 (b).

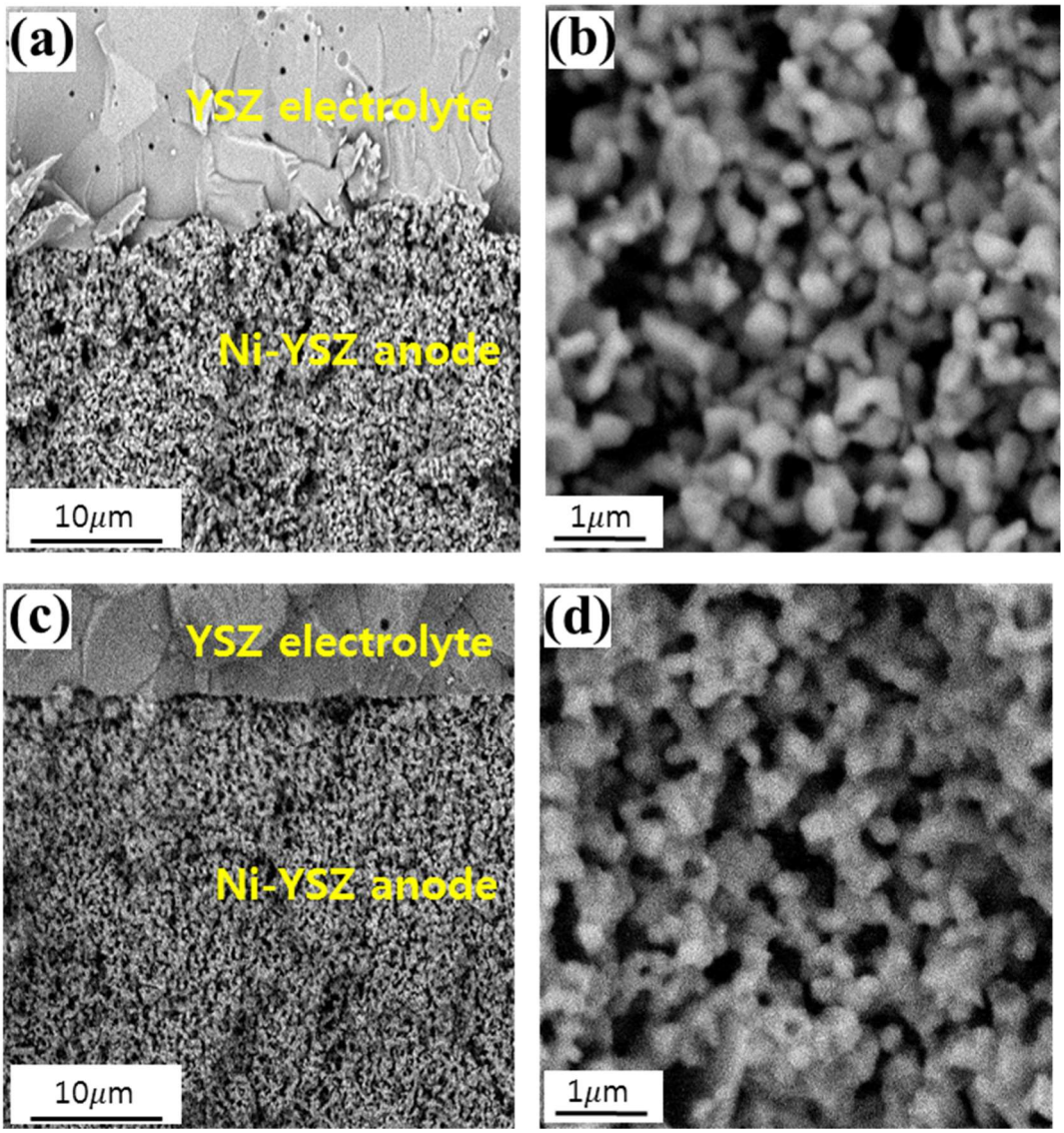

Fig. 5.7. Microstructures of Ni-YSZ anodes after electrochemical tests. (a) and (b) SEM images of Ni-YSZ anode (W10N10). (c) and (d) SEM images of Ni-YSZ anode (W0N20).

6. Conclusions

Homogeneously distributed NiO-YSZ nanocomposite particles for nanostructured anode were synthesized successfully by the W/O micro-emulsion method. The particle size of NiO-YSZ powders synthesized by micro-emulsion, calcined at 500 ºC was around 40 nm. Electrochemical performances were improved by the nanocomposite anode synthesized by micro-emulsion, compared with the results obtained by the conventional anode. A single cell with micro-emulsion synthesized Ni-YSZ anode showed a higher maximum power density, 359 mW cm^{-2}, compared with that of a single cell with conventional Ni-YSZ anode, 204 mW cm^{-2}, at the operating temperature of 850 ºC. The electrode resistance of a single cell decreased to 0.44 Ω cm^2 with micro-emulsion synthesized anode, compared with the value of a conventional cell, 1.14 Ω cm^2, at the same operating temperature with I-V analysis. The electrochemical performance of a single cell was improved by the enlarged TPB obtained by the micro-emulsion synthesized Ni-YSZ anode composed of uniformly distributed nano-grains. Further studies to optimize the micro-emulsion procedures showed the anode morphology like particle size was affected by controlling the alkali concentrations. Three types of micro-emulsion synthesized NiO-YSZ powders, W10N10, W5N15, and W0N20, with different alkali concentrations, were discussed. Particle size of W0N20 decreased to 30nm compared with the value of W10N10, around 40nm. Moreover, specific surface area of W0N20 drastically increased to 42.27 m^2/g, from the value of W10N10, 14.98 m^2/g. However, the maximum power density of a single cell was not affected by the alkali concentrations. The electrode resistance of a single cell with W0N20 showed a higher value of 0.65 Ω cm^2, compared with the value of a single cell with W10N10, 0.44 Ω cm^2, at the open circuit voltage with the operating temperature of 850 ºC, although the particle size of W0N20 is smaller than that of W10N10. The reduced TPB length caused by the agglomeration of too small particles might be the reason of the electrochemical performances of single cells.

REFERENCES

[1] N. Q. Minh, *J. Am. Ceram. Soc*. **1993**, 76, 563.

[2] Z. S. Duan, M. Yang, A. Y. Yan, Z. F. Hou, Y. L. Dong, Y. Chong, M. J. Cheng, W. S. Yang, *J. Power Sources* **2006**, 160, 57.

[3] K. T. Lee, E. D. Wachsman, *Science* **2011**, 334, 935.

[4] P. Singh, J. B. Goodenough, *J. Am. Chem. Soc*. **2013**, 135, 10149.

[5] H. Moon, S. D. Kim, S. H. Hyun, H. S. Kim, *Int. J. Hydrogen Energy* **2008**, 33, 1758.

[6] Z. P. Shao, S. M. Haile, *Nature* **2004**, 431, 170.

[7] T. Suzuki, Z. Hasan, Y. Funahashi, T. Yamaguchi, Y. Fujishiro, M. Awano, *Nature* **2009**, 325, 852.

[8] A. Yan, M. Phongaksorn, D. Nativel, E. Croiset, *J. Power Sources* **2012**, 210, 374.

[9] S. Primdahl, M. Mogensen, *J. Electrochem. Soc*. **1997**, 144, 3409.

[10] Z. P. Shao, W. Zhou, Z. H. Zhu, *Prog. Mater. Sci*. **2012**, 57, 804.

[11] S. P. Jiang. Y. Y. Duan, J. G. Love, *J. Electrochem. Soc*. **2002**, 149, 1175.

[12] V. Esposito, D. Z. Florio, E. N. S. Muccillo, R. Muccillo, E. Traversa, *J. Eur. Ceram. Soc*. **2005**, 25, 2637.

[13] S. H. Chan, Z. T. Xia, *J. Electrochem. Soc*. **2001**, 4, 388.

[14] M. Brown, S. Primdahl, M. Mogensen, *J. Electrochem. Soc*. **2000**, 147, 475.

[15] K. Yamamoto, T. Hashishin, M. Matsuda, N. Qiu, Z. Tan, S. Ohara, *Nano Energy* **2014**, 6, 103.

[16] M. K. Rath, M. J. Lee, K. T. Lee, *Ceram. Int*. **2014**, 40, 1909.

[17] C. M. Grgicak, R. G. Green, W. F. du, *J. Am. Ceram. Soc*. **2005**, 88, 308.

[18] X. Xi, H. Abe, K. Kuruma, R. Harada, A. Shui, M. Naito, *Advanced Powder Technology* **2014**, 25, 490.

[19] P. G. Keech, D. E. Trifan, V. I. Birss, *J. Electrochem. Soc*. **2005**, 152, 645.

[20] S. D. Kim, H. Moon, S. H. Hyun, J. Moon, J. Kim, H. W. Lee, *J. Power Sources* **2006**, 163, 392.

[21] X. L, Weng, D. Brett, V. Yufit, *Solid State Ion* **2010**, 181, 827.

[22] P. Duran, J. Tarta, F. Capel, *J. Eur. Ceram. Soc*. **2003**, 23, 2125.

[23] B. K. Paul, S. P. Moulik, *Current Science* **2001**, 990.

[24] W. C. Chueh, Y. Hao, W. C. Jung, S. M. Haile, *Nature Materials* **2012**, 11, 155.

[25] M. Liu, S. Wang, T. Chen, C. Yuan, Y. Zhou, S. Wang, J. Huang, *J. Power Sources* **2015**, 274, 730.

[26] K. Chen, X. Chen, Z. Lu, N. Ai, X. Huang, W. Su, *Electrochim. Acta*. **2008**, 53, 7825.

[27] D. Yoon, J. J. Lee, H. G. Park, S. H. Hyun, *J. Electrochem. Soc*. **2010**, 157, B455.

[28] N. Ai, Z. Lu, K. Chen, X. Huang, X. Du, W. Su, *J. Power Sources* **2007**, 171, 489.

[29] Z. Gao, E. C. Miller, S. A. Barnett, *Adv. Funct. Mater*. **2014**, 24, 5703.

[30] Y. Zhou, H. Wu, T. Luo, J. Wang, Y. Shi, C. Xia, S. Wang, Z. Zhan, *Adv. Energy Mater*. **2015**, 5, 1500375.

[31] K. Sato, G. Okamoto, M. Naito, H. Abe, *J. Power Sources* **2009**, 193, 185.

[32] X. Xi, A. Kondo, M. Naito, *J. Alloys and Compounds* **2016**, 688, 1047.

요약문

W/O 마이크로에멀젼을 통한 나노컴퍼지트 Ni-YSZ 음극 제조와 고체산화물 연료전지의 성능 향상을 위한 알칼리 농도의 최적화

고체산화물 연료전지의 음극 제조를 위해 활용될 균일하게 분산된 나노복합체의 NiO-YSZ 파우더가 W/O 마이크로에멀젼을 통하여 제조되었다. W/O 마이크로에멀젼을 통해 제조된 파우더는 입자크기가 50 nm 이하인 미세한 구조를 가지는 것으로 확인되었다. 동시에 마이크로에멀젼으로 제조한 파우더에 불순물 상이 존재하지 않는 것을 확인할 수 있었다. 이후, 마이크로에멀젼을 통해 나노복합체 Ni-YSZ 음극을 제조하였고, 제조된 결과물이 고체산화물 연료전지의 성능에 미치는 영향을 확인하였다. 850도의 작동 온도에서 마이크로에멀젼을 통해 제조된 Ni-YSZ 음극으로 구성된 연료전지의 MPD는 359 mW/cm^2 으로 확인되었고, 이는 단순히 기계적으로 볼밀링 과정을 통해 제조된 Ni-YSZ 음극으로 구성된 연료전지가 가지는 204 mW/cm^2 에 비해 크게 향상된 값이다. 같은 작동 온도에서 연료전지의 전극 저항을 확인하였을 때, 마이크로에멀젼을 통해 제조된 연료전지는 0.44 Ωcm^2, 볼밀링 과정을 통해 제조된 연료전지는 1.14 Ωcm^2의 값을 보이는 것을 확인하였다. 마이크로에멀젼을 통해 제조된 Ni-YSZ 음극은 균일하게 분산되어 있는 나노입계로 구성되어있고, 그로 인한 삼상계면의 증가가 연료전지의 전기화학적 성능의 향상을 가져온 것으로 여겨진다. 추가적으로, 보다 더 미세한 NiO-YSZ 파우더를 제조하고, 그를 통한 고체산화물 연료전지의 전기화학적 특성을 향상시키기 위해 알칼리 용액 농도를 조정하는 마이크로에멀젼의 최적화 과정을 진행하였다. 마이크로에멀젼을 통해 제조된 세 가지 종류의 NiO-YSZ 파우더인 W10N10, W5N15,

W0N20을 다루었다. 먼저, 알칼리 용액의 농도가 진해짐에 따라 NiO-YSZ 파우더의 입자 크기가 더욱 작아지는 것을 확인하였다. 알칼리 농도가 가장 진한 W0N20 파우더의 경우 입자 크기가 30nm 정도까지 작아진 것을 확인하였다. 동시에 비표면적 또한 알칼리의 농도가 진해짐에 따라 증가하는 것을 확인할 수 있었다. 세 가지의 알칼리 농도에 따라 제조된 NiO-YSZ 파우더 모두, 불순물 상이 존재하지 않는 것을 확인하였다. 제조된 파우더를 활용하여 나노복합체 Ni-YSZ로 구성된 고체산화물 연료전지를 제조하였고, 알칼리 농도를 변화시키는 것이 고체산화물 연료전지의 성능에 미치는 영향을 확인하였다. 알칼리 농도가 변화함에 따라 파우더의 입자 크기와 같은 음극의 미세 구조가 달라지는 것을 확인하였으나, 연료전지의 MPD 값은 알칼리 농도에 거의 영향을 받지 않는 것으로 확인되었다. 연료전지의 전극 저항을 확인하였을 때에는 오히려, 입자 크기가 더 작은 W0N20으로 구성된 전지의 저항인 0.65 Ωcm^2이 W10N10으로 구성된 전지의 0.44 Ωcm^2에 비해 더 큰 값을 보이는 것을 확인할 수 있었다. W0N20 파우더의 너무 작은 입자들의 경우 서로 뭉쳐지려는 경향이 더 크게 나타나게 되고, 그로 인한 삼상계면의 감소가 연료전지의 성능을 오히려 저하시킨 것으로 생각하였다.

핵심어: 고체산화물 연료전지, 나노복합체, Ni-YSZ, W/O 마이크로에멀젼, 알칼리 농도.